ANALYTICAL AND NUMERICAL STUDY OF DIFFUSIVE FLUXES FOR TRANSPORT EQUATIONS WITH NEAR-DEGENERATE COEFFICIENTS

J. PROFT* AND B. RIVIÈRE†

Abstract. This work formulates and analyzes a new family of discontinuous Galerkin methods for the convection-diffusion equation with highly varying diffusion coefficients, that do not require the use of slope limiting techniques. The proposed methods are based on the standard NIPG/SIPG techniques, but use special diffusive numerical fluxes at some important interfaces. The resulting numerical solutions do not show any overshoot or oscillation phenomena. Error analysis and numerical examples are provided.

Key words. numerical fluxes, discontinuous Galerkin methods, high and low diffusivity

1. Introduction and Problem Definition. In this work we explore the development and analysis of discontinuous Galerkin methods applied to the solution of linear advection-diffusion equations

$$\partial_t u + \nabla \cdot (\beta u - \epsilon \nabla u) = f, \qquad \text{in} \quad \Omega \times (0,T). \tag{1.1}$$

Although problems of this type occur in many applications, we are primarily motivated by the modeling of flow in porous media such as petroleum reservoir and groundwater aquifer simulation [4, 7, 16]. Here, the physical, geological, and chemical properties of the medium may lead to a degeneracy in the spatially dependent diffusion coefficient of the mathematical equations describing the model.

A major difficulty associated with such problems is the lack of mathematical regularity of the solution in the degenerate diffusion case. Moreover, classical numerical methods exhibit instability in the solution even in the non-degenerate case, when the diffusion coefficient is sufficiently small compared to the advection coefficient to render the numerical solution incapable of capturing the resulting boundary layer phenomena. In such a situation, the local Peclet number, which reflects the ratio of advection to diffusion, is sufficiently high to impose hyperbolic-type behavior in the solution. Although this phenomena may be resolved by refinement of the mesh, there is a corresponding considerable increase in computational effort.

Equations of this type have been discretized using classical finite element and finite difference methods that typically utilize an operator splitting technique to handle the difficulties associated with advective transport and diffusion separately [26, 21]. Such computational methods often utilize slope limiting procedures to supress the amount of unphysical oscillations in the numerical solution [7] or the inclusion of a streamline-diffusion stabilization term [20]. Additionally, domain decomposition techniques utilizing differing numerical methods on distinct subdomains have been proposed to model the multi-physics aspects of the problem [17, 30]. In this paper, we propose an adaptive flux technique to maintain stability, based on a discontinuous Galerkin (DG) discretization, that makes the use of slope limiting techniques superfluous.

*Department of Mathematics, The University of Texas at Austin, Austin, TX 78712 (proft@ices.utexas.edu)

†Department of Mathematics, University of Pittsburgh Pittsburgh, PA 15260 (riviere@math.pitt.edu). This author is partially supported by grant NSF DMS 0506039

DG methods possess several characteristics which render them useful in many applications. The flexibility of the method allowsfor element-wise polynomial degree approximation and general non-conforming meshes. Some well known versions applied to elliptic equations include the symmetric interior penalty method proposed by Arnold [2], the OBB method of Oden, Babuskaand Baumann [3], and the non-symmetric interior penalty Galerkin method (NIPG) of Rivière, Wheeler and Girault [24, 25]. In [19], Houston, Schwab and Suli extend the analysis to avection-diffusion-reaction problems. Recently, Wheeler, Dawson and Sun [12] propose an incomplete interior penalty version (IIPG) to address incompatibility for coupled flow and transport problems. DG methods have been applied to transport equations [23, 29] where the estimates derived are semi-discrete and present numerical examples for constant diffusion only. In the context of coupled transport and miscible displacement, several examples have been recently explored by Dawson, Sun, Rivière and Wheeler [12, 27, 22, 28]. Alternative DG methods based on the discretization of hyperbolic equations include the local discontinous Galerkin method of Cockburn and Shu [9], subsequently extended to advection-diffusion equations in [11, 6, 1]. The case of a spatially dependent, possibly degenerate diffusion coefficient has not been analyzed previously in the context of DG methods. Our work focuses on the symmetric and non-symmetric interior penalty versions and explores various flux definitions to analyze the stability of the resulting method, particularly on the interfaces from high to low diffusivity, that results in a novel and highly successful adaptive technique. Moreover, our analysis, which depends on the spatially varying diffusion coefficient, is valid even in the case of degenerate diffusion (purely hyperbolic behavior). In the following section, we define the formulation of our semi-discrete scheme. Error estimates are proved in Section 3. Both implicit and explicit fully discrete schemes are analysed in Section 4. Section 5 contains the adaptive scheme and corresponding analysis. Finally numerical examples are presented in Section 6.

In the following section, we define the formulation of our semi-discrete scheme. Error estimates are proved in Section 3. Both implicit and explicit fully discrete schemes are analysed in Section 4. Section 5 contains the adaptive scheme and corresponding analysis. Finally numerical examples are presented in Section 6.

2. Formulation. The specific equation we consider is of advection-diffusion type defined on a bounded polygonal domain Ω in $\mathbb{R}^d$, $d = 1, 2, 3$,

$$\partial_t u + \nabla \cdot (\beta u - \epsilon \nabla u) = f, \qquad \text{in} \quad \Omega \times (0, T), \tag{2.1}$$

supplemented with boundary and initial conditions

$$u(x,t) = u_0(x), \qquad x \in \Omega, t = 0, \tag{2.2}$$

$$(\beta u(x,t) - \epsilon \nabla u(x,t)) \cdot n_{\partial\Omega} = \beta u_{\text{in}} \cdot n_{\partial\Omega}, \qquad x \in \partial\Omega_{\text{in}},\ t \geq 0, \tag{2.3}$$

$$-\epsilon \nabla u(x,t) \cdot n_{\partial\Omega} = 0, \qquad x \in \partial\Omega_{\text{out}},\ t \geq 0, \tag{2.4}$$

where $u_0, u_{\text{in}} \in L^2(\Omega)$. We assume that the velocity $\beta \in \mathbb{R}^d$ is divergent-free: $\nabla \cdot \beta = 0$. Define inflow and outflow regions $\partial\Omega_{\text{in}} = \{x \in \partial\Omega : \beta \cdot n_{\partial\Omega} < 0\}$ and $\partial\Omega_{\text{out}} = \{x \in \partial\Omega : \beta \cdot n_{\partial\Omega} \geq 0\}$ respectively. The unit vector $n_{\partial\Omega}$ is outward to the boundary $\partial\Omega$.

We assume that the spatially dependent function $\epsilon = \epsilon(x)$ is bounded in Ω uniformly: $0 \leq \epsilon_* \leq \epsilon \leq \epsilon^*$. In general, ϵ may vary over the domain with several orders of magnitude. We denote by Ω_H the region of Ω for which $\epsilon = \epsilon_H$ is smaller (for example $\epsilon_H = \mathcal{O}(10^{-4})$) and by Ω_P the region for which $\epsilon = \epsilon_P$ is larger (for example $\epsilon_P = \mathcal{O}(1)$). Let Γ define the interface between regions where $\epsilon = \epsilon_H$, imposing

hyperbolic-type solution behavior, and $\epsilon = \epsilon_P$, imposing parabolic-type solution behavior. Conventionally set the unit normal n_Γ on Γ to face outward from $\Omega_{\rm P}$ and inward to $\Omega_{\rm H}$. Define $\Gamma_{\rm HP}$ to be the subset of Γ through which the flow crosses from hyperbolic to parabolic subdomains:

$$\Gamma_{\rm HP} = \{x \in \Gamma : \beta \cdot n_\Gamma < 0\}.$$

The accurary of the numerical solution at the interface from low to high diffusivity (and not vice-versa) is of primary interest, since the numerical solution may exhibit instability resulting in overshoot or oscillations at this location.

In the limiting case where $\epsilon = 0$ on Ω_H, continuity of the flux must hold across any purely hyperbolic and parabolic interface, whereas continuity of the solution needs to be satisfied only on the subset $\Gamma_{\rm HP}$ [18]. Although the flow is continuous elsewhere in the domain, at this interface there is a jump discontinuity in the normal derivative of the solution so that a standard NIPG analysis would no longer apply. Even in the case where diffusion is nonzero but small, the numerical solution mimics this limiting case and may exhibit overshoot on $\Gamma_{\rm HP}$ [14]. Consequently, we discretize the advection-diffusion equation via DG interior penalty techniqes and explore strategies for defining stable numerical flux functions on $\Gamma_{\rm HP}$.

Let $\mathcal{T}_h = \{\Omega_e\}_e$ be a nondegenerate subdivision of Ω such that $\Gamma_{\rm HP}$ is the union of a subset of edges in 2D (and faces in 3D). In other words, an element Ω_e is either a subset of Ω_H or a subset of Ω_P. As usual, we denote h_e to be the diameter of element Ω_e and h the maximum diameter of elements in $\mathcal{T}_h$. Let F_h be the set of faces belonging to elements $\Omega_e \in \mathcal{T}_h$ and partition F_h into distinct sets $F^i_{\rm HP} \cup F^i \cup F^\partial_{\rm in} \cup F^\partial_{\rm out}$, where $F^i_{\rm HP}$ denotes the set of interior faces on interface region $\Gamma_{\rm HP}$, F^i denotes the set of remaining interior faces, $F^\partial_{\rm in}$ the set of faces located on $\partial\Omega_{\rm in}$, and $F^\partial_{\rm out}$ the set of faces located on $\partial\Omega_{\rm out}$. To each face $F \in F_h$, we associate a unit normal vector n_F such that n_F coincides with $n_{\partial\Omega}$ on $F^\partial_{\rm in} \cup F^\partial_{\rm out}$ and with n_Γ on $F^i_{\rm HP}$.

Let p be a positive integer. Define the finite element approximating space

$$V_h = \{v_h \in L^2(\Omega) : \forall \Omega_e \in \mathcal{T}_h(\Omega), v_h|_{\Omega_e} \in \mathbb{P}^p(\Omega_e)\},$$

where $\mathbb{P}^p(\Omega_e)$ is the set of polynomials of total degree less than p. Let $(\cdot,\cdot)_{\Omega_e}$ and $\langle\cdot,\cdot\rangle_F$ denote the L^2 inner-product over $\Omega_e \in \mathcal{T}_h$ and $F \in F_h$ respectively. The corresponding L^2 norm is denoted by $\|\cdot\|_{\Omega_e}$ or $\|\cdot\|_F$. Let $H^k(\Omega)$ be the standard Sobolev space with norm $\|\cdot\|_{H^k(\Omega)}$ and semi-norm $|\cdot|_{H^k(\Omega)}$. Let $L^2(0,T;H^k(\Omega))$ denote the space of functions v with $\int_0^T \|v(t)\|^2_{H^k(\Omega)} < \infty$. For any interior face $F = \partial\Omega_{e_1} \cap \partial\Omega_{e_2}$ with n_F pointing from Ω_{e_1} to Ω_{e_2}, we define the jump [] and average operators {}:

$$\forall v_h \in V_h, \quad [v_h] = v_h|_{\Omega_{e_1}} - v_h|_{\Omega_{e_2}}, \quad \{v_h\} = 0.5(v_h|_{\Omega_{e_1}} + v_h|_{\Omega_{e_2}}).$$

We also define upwind and downwind quantities, using characteristic functions $1_{\{\}}$:

$$v_F^\uparrow = v|_{\Omega_{e_1}} 1_{\{\beta\cdot n_F \geq 0\}} + v|_{\Omega_{e_2}} 1_{\{\beta\cdot n_F < 0\}}, \quad v_F^\downarrow = v|_{\Omega_{e_1}} 1_{\{\beta\cdot n_F < 0\}} + v|_{\Omega_{e_2}} 1_{\{\beta\cdot n_F \geq 0\}}. \quad (2.5)$$

For $u_h, v_h \in V_h$, define the bilinear form

$$\begin{aligned} A(u_h, v_h) = &- \sum_{\Omega_e \in \mathcal{T}_h} (\beta u_h - \epsilon \nabla u_h, \nabla v_h)_{\Omega_e} + \sum_{F \in F^i} |F|^{-1} \langle \sigma_F [u_h], [v_h] \rangle_F \\ &+ \sum_{F \in F^i} \langle \beta u_h^{\uparrow} \cdot n_F, [v_h] \rangle_F + \sum_{F \in F^{\partial}_{\text{out}}} \langle \beta u_h \cdot n_F, v_h \rangle_F \\ &- \sum_{F \in F^i} \langle \{\epsilon \nabla u_h\} \cdot n_F, [v_h] \rangle_F + \kappa \sum_{F \in F^i} \langle \{\epsilon \nabla v_h\} \cdot n_F, [u_h] \rangle_F \\ &+ a(u_h, v_h) + d(u_h, v_h), \end{aligned} \tag{2.6}$$

and linear form

$$L(v_h) = (f, v_h)_{\Omega} - \sum_{F \in F^{\partial}_{\text{in}}} \langle \beta u_{\text{in}} \cdot n_F, v_h \rangle_F. \tag{2.7}$$

The coefficient κ takes the value $+1$ or -1, which yields the non-symmetric (resp. symmetric) interior penalty Galerkin method except on the interface Γ_{HP}. The penalty parameter σ_F may vary from face to face, but for simplicity of the writing we might drop the subscript F and use the notation σ. We will choose σ to be equal to 1 if $\kappa = 1$ (non-symmetric case) and bounded below by a large enough constant σ_0 if $\kappa = -1$ (symmetric case) (see [15]). Here, $|F|$ denotes the $(d-1)$-dimensional measure of F. One aim of this paper is to study numerically and theoretically different approaches for defining the advective interface term $a(\cdot, \cdot)$ and diffusive interface term $d(\cdot, \cdot)$ on Γ_{HP}. The following numerical fluxes are considered:

$$\begin{aligned} a(u_h, v_h) = a_1(u_h, v_h) &= \sum_{F \in F^i_{\text{HP}}} \langle (\beta u_h)^{\uparrow} \cdot n_F, [v_h] \rangle_F, \\ a(u_h, v_h) = a_2(u_h, v_h) &= \sum_{F \in F^i_{\text{HP}}} \langle \{\beta u_h\} \cdot n_F, [v_h] \rangle_F, \\ a(u_h, v_h) = a_3(u_h, v_h) &= \sum_{F \in F^i_{\text{HP}}} \langle (\beta u_h)^{\downarrow} \cdot n_F, [v_h] \rangle_F, \\ d(u_h, v_h) = d_1(u_h, v_h) &= -\delta\nu(u_h, v_h) + \tilde{\kappa}\delta\nu(v_h, u_h), \\ d(u_h, v_h) = d_2(u_h, v_h) &= -\delta\nu(u_h, v_h) + \tilde{\kappa}\delta\nu(v_h, u_h) + j_{\tilde{\sigma}}(u_h, v_h), \\ d(u_h, v_h) = d_3(u_h, v_h) &= -\alpha(u_h, v_h) + \tilde{\kappa}\alpha(v_h, u_h) + j_{\tilde{\sigma}}(u_h, v_h), \\ d(u_h, v_h) = d_4(u_h, v_h) &= -\sum_{F \in F^i_{\text{HP}}} \langle (\epsilon \nabla u_h)^{\downarrow}, [v_h] \rangle_F, \end{aligned}$$

where we have

$$\begin{aligned} \nu(u_h, v_h) &= \sum_{F \in F^i_{\text{HP}}} \langle (\epsilon \nabla u_h)^{\uparrow} \cdot n_F, [v_h] \rangle_F, \\ \alpha(u_h, v_h) &= \sum_{F \in F^i_{\text{HP}}} \langle \{\epsilon \nabla u_h\} \cdot n_F, [v_h] \rangle_F, \\ j_{\tilde{\sigma}}(u_h, v_h) &= \sum_{F \in F^i_{\text{HP}}} |F|^{-1} \langle \tilde{\sigma} [u_h], [v_h] \rangle_F. \end{aligned}$$

The parameters δ and $\tilde{\kappa}$ take the values: $\delta \in [0,1]$ and $\tilde{\kappa} \in \{-1,0,+1\}$. The penalty parameter $\tilde{\sigma}$ will be defined later; it could be the constant 1 or else a large constant $\tilde{\sigma}_0$ or else equal to the function ϵ_H. The fluxes a_1, a_2 and a_3 correspond to upwinding, averaging and downwinding the advective term respectively. We will show numerically that only the case a_1 yields accurate solutions, whereas the case a_3 produces unstable solutions. The fluxes d_1, d_2 and d_3 correspond to the diffusive term. The first two choices are two versions of an upwinding diffusive flux: the flux is stabilized by the addition of either a jump term or a symmetric/non-symmetric term. The choice d_3 is the standard interior penalty Galerkin flux (see [23]) if $\tilde{\sigma}$ is nonzero. If both $\tilde{\sigma}$ and $\tilde{\kappa}$ are zero, the case $d = d_3$ is the averaged diffusive flux. Finally, the case $d = d_4$ is a downwinded diffusive flux; this choice produces large amounts of overshoot/oscillations.

For any $t > 0$, the continuous in time solution $u_h(t) \in V_h$ of (2.1) satifies

$$\forall v_h \in V_h, \quad (\partial_t u_h, v_h)_\Omega + A(u_h(t), v_h) = L(v_h), \tag{2.8}$$

$$\forall v_h \in V_h, \quad (u_h(0), v_h)_\Omega = (u_0, v_h)_\Omega. \tag{2.9}$$

The formulation (2.8) is obtained from the differential equation (2.1) using standard techniques: (2.1) is multiplied by a test function $v_h \in V_h$, integrated by parts over one element Ω_e and the resulting equation is summed over all elements. The boundary integrals are transformed into a summation of edge integrals (see [23]).

Our investigation of various flux functions defined on Γ_{HP} is motivated by the numerical instabilities of the computed solution when the diffusion coefficient on Ω_H is very small. In the limiting case $\epsilon = 0$ on Ω_H, the interface conditions are relatively well understood. In [18], Gastaldi and Quarteroni employ a vanishing viscosity singular perturbation analysis to derive appropriate theoretical interface conditions: continuity of the flux must hold across any hyperbolic and parabolic interface, whereas continuity of the solution needs to be satisfied only on the subset Γ_{HP}. We remark that Croiseille et al. [10] have used these interface conditions to establish well-posedness of a one dimensional periodic degenerate diffusion advection-diffusion equation. These conditions were numerically verified by Ern and Proft [14] who additionally demonstrate that for a nonvanishing but small ϵ_H, the corresponding fluxes $(a,d) = (a_1, 0)$ yield a stable solution without overshoot/oscillations whereas the standard choice $(a,d) = (a_1, d_3)$ with $\tilde{\sigma} = \tilde{\kappa} = 1$ produces a faulty solution with overshoot.

Figures 2.1 and 2.2 present a numerical example without the use of slope limiters for which $\beta = (1,0), \epsilon_P = 1$ and $\epsilon_H = 10^{-3}$. The problem is described in detail in Section 6.1, and is indicative of the numerical difficulties associated with large local Peclet numbers:

$$Pe = \frac{\|\beta\|_{L_\infty} h}{2\epsilon} > 1. \tag{2.10}$$

The mesh is defined in Fig. 2.1 with gray areas indicating Ω_H and white areas Ω_P. Fig. 2.2(a) displays the standard NIPG solution with overshoot near Γ_{HP} and Fig. 2.2(b) an improved solution with flux $d = 0$ along the line $y = 0.25$. In what follows, we will give a theoretical explanation of these numerical behaviors. We will also investigate other choices for the diffusive flux.

3. Analysis. In this section we analyze the scheme (2.8)-(2.9) with $a = a_1$ and $d = d_1, d_2, d_3$. We prove stability bounds, then state the consistency of the scheme and derive some error estimates. We first define two conditions that may be assumed to hold for certain choices of the diffusive flux.

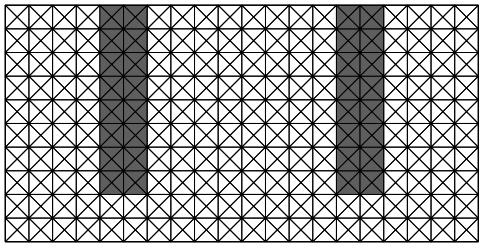

FIG. 2.1. *Mesh and domain partition of hyperbolic-type subdomains where* $\epsilon_H = 10^{-3}$ *(gray) and parabolic-type subdomain where* $\epsilon_P = 1$ *(white).*

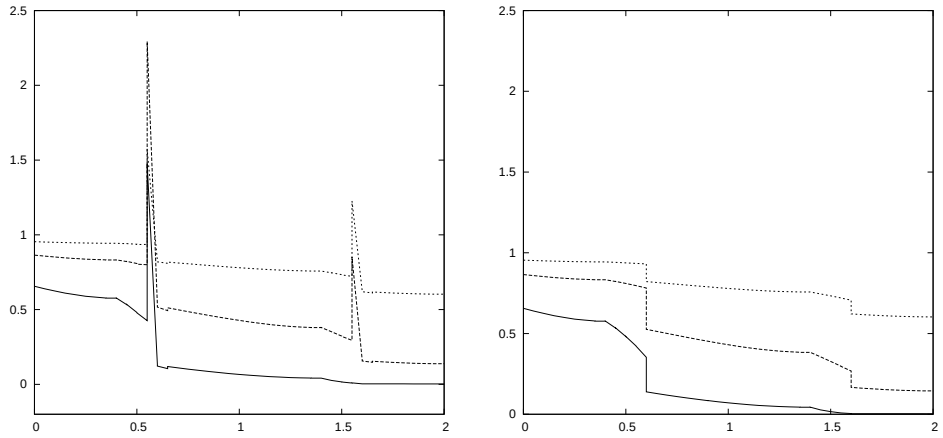

FIG. 2.2. *(a) Explicit NIPG solution* ($d = d_3$ *and* $\kappa = \tilde{\kappa} = \sigma_F = \tilde{\sigma} = 1$*); (b) Explicit NIPG solution* ($\kappa = \sigma_F = 1$*) with upwind advective flux and zero diffusive flux* $d = 0$*, at times* t_0 *(solid line),* t_1 *(dashed line) and* t_2 *(dotted line).*

Condition I: The parameter $\tilde{\sigma}$ is equal to a sufficiently large enough constant $\tilde{\sigma}_0$.

Condition II: Assume that

$$0 \leq \delta \sqrt{\epsilon_H^{\Delta}} < h, \tag{3.1}$$

where Δ_H denotes the set of elements $\Omega_e \subset \Omega_H$ such that the intersection $\partial\Omega_e \cap F_{\mathrm{HP}}^i$ contains at least one edge (or face) and $\epsilon_H^{\Delta} = \max_{x \in \Delta_H} \epsilon_H(x)$.

Let us define for $k = 1, 2, 3$, the norms $|||\cdot|||$ and $|||\cdot|||_k$:

$$\begin{aligned} |||v_h|||^2 = &\sum_{\Omega_e \in \mathcal{T}_h} \|\epsilon^{1/2} \nabla v_h\|_{\Omega_e}^2 + \sum_{F \in F^i \cup F_{\mathrm{HP}}^i} \||\beta \cdot n_F|^{1/2} [v_h]\|_F^2 \\ &+ \sum_{F \in F_{\mathrm{in}}^{\partial} \cup F_{\mathrm{out}}^{\partial}} \||\beta \cdot n_F|^{1/2} v_h\|_F^2 + \sum_{F \in F^i} |F|^{-1} \|\sigma_F^{1/2} [v_h]\|_F^2, \end{aligned} \tag{3.2}$$

$$|||v_h|||_1 = |||v_h|||, \quad |||v_h|||_2 = |||v_h|||_3 = (|||v_h|||^2 + j_{\tilde{\sigma}}(v_h, v_h))^{1/2}. \tag{3.3}$$

Note that $|||\cdot|||_1$ is the energy norm corresponding to the case $d = d_1$ whereas $|||\cdot|||_2$ and $|||\cdot|||_3$ correspond to $d = d_2$ and $d = d_3$ respectively.

3.1. Analysis Tools. In subsequent analysis, we will use the following trace inequalities with respect to $h_e = \mathrm{diam}(\Omega_e)$ [2]:

$$\forall v \in H^1(\Omega_e), \quad \|v\|_F^2 \leq C_e^t \Big(\frac{1}{h_e} |v|_{\Omega_e}^2 + h_e |v|_{H^1(\Omega_e)}^2 \Big), \tag{3.4}$$

$$\forall v \in H^2(\Omega_e), \quad \|\nabla v \cdot n_F\|_F^2 \leq C_e^t \Big(\frac{1}{h_e} |v|_{H^1(\Omega_e)}^2 + h_e |v|_{H^2(\Omega_e)}^2 \Big). \tag{3.5}$$

Define trace constant $C_t = \max_{\Omega_e \in \mathcal{T}_h} C_e^t$. For polynomial functions, we use the following trace lemma [25]:

LEMMA 3.1. *For element Ω_e in $\mathbb{R}^n$, $(n = 2, 3)$ with $h_e = \mathrm{diam}(\Omega_e)$, let F be an edge or a face of Ω_e with unit normal vector n_F. Then, if v_h is a finite polynomial on Ω_e, there exists a constant C_e^τ independent of Ω_e such that*

$$\|v_h\|_F \leq C_e^\tau h_e^{-1/2} \|v_h\|_{\Omega_e}, \tag{3.6}$$

$$\|\nabla v_h \cdot n_F\|_F \leq C_e^\tau h_e^{-1/2} \|\nabla v_h\|_{\Omega_e}. \tag{3.7}$$

Define trace constant $C_\tau = \max_{\Omega_e \in \mathcal{T}_h} C_e^\tau$. We assume that $\{\mathcal{T}_h\}_{h>0}$ is such that C_t and C_τ can be bounded by a finite constant uniformly in h. Recall the standard inverse inequality, valid for piecewise polynomials on shape-regular families of triangulations [5, 13]: There exists a constant C_i independent of Ω_e such that for any v_h finite polynomial on Ω_e

$$\|v_h\|_{H^1(\Omega_e)} \leq C_i h_e^{-1} \|v_h\|_{\Omega_e}. \tag{3.8}$$

We will have occasion to use the continuous interpolant $u^*(t) \in V_h \cap \mathcal{C}^0(\Omega)$ of $u(t)$ that satisfies the following approximation properties: For $q = 0, 1, 2$,

$$\forall t \in (0, T), \quad \|u(t) - u^*(t)\|_{H^q(\Omega)} \leq C_a h^{p+1-q} |u(t)|_{H^{p+1}(\Omega)}. \tag{3.9}$$

$$\forall t \in (0, T), \quad \|\partial_t u(t) - \partial_t u^*(t)\|_{\Omega} \leq C_a h^{p} |\partial_t u(t)|_{H^{p}(\Omega)}. \tag{3.10}$$

Recall the following form of Gronwall's lemma [5]: Let g and ρ be continuous non-negative functions defined on an interval $a \leq t \leq b$, ρ being also non-decreasing. If for $t \in [0, b]$, $g(t) + h(t) \leq \rho(t) + \int_a^t g(s) ds$, then $g(t) + h(t) \leq C_g \rho(t)$ with $C_g = \exp(t - a)$. Additionally, Young's inequality will prove useful in our analysis: For real numbers a, b and for $\gamma > 0$, $ab \leq \frac{\gamma}{2} a^2 + \frac{1}{2\gamma} b^2$.

Finally, we will use the constant C throughout the paper for a generic constant independent of h, ϵ and δ, unless specified otherwise. We will also explicitely add to the constant the parameters on which this constant depends: for instance, the constant $C_{i,\tau,\sigma}$ depends on C_i, C_τ, and σ.

3.2. Stability and Consistency. In this section, we derive stability bounds for the proposed schemes and determine consistency.

THEOREM 3.2. *Let u_h be the semi-discrete solution in V_h to (2.8)-(2.9) and assume that $a = a_1$ and for given $k = 1, 2, 3$, fix $d = d_k$. Then u_h satisfies the bound:*

$$\|u_h(T)\|_\Omega^2 + \int_0^T |||u_h(t)|||_k^2 dt \leq \|u_h(0)\|_\Omega^2 + C_{\tau,\epsilon^*} \int_0^T (\|f\|_\Omega^2 + \sum_{F \in F_{\mathrm{in}}^\partial} \||\beta \cdot n_F|^{1/2} u_{\mathrm{in}}\|_F^2) dt. \tag{3.11}$$

where C_{τ,ϵ^*} is a constant independent of h and ϵ_* but dependent on C_τ and ϵ^* whenever $\delta \neq 0$. This stability bound holds unconditionally except in the following cases where either Condition I or Condition II is needed:

- $k = 3, \tilde{\kappa} \in \{-1, 0\}$ *and Condition I.*
- $k = 1, \delta \neq 0, \tilde{\kappa} \in \{-1, 0\}$ *and Condition II.*
- $k = 2, \delta \neq 0, \tilde{\kappa} \in \{-1, 0\}$ *and Condition I.*

Proof. Fix $t > 0$. To simplify notation, we write $u_h(t) = u_h$. Using Green's formula and the fact that $\nabla \cdot \beta = 0$, we have [8]:

$$-\sum_{\Omega_e \in \mathcal{T}_h} (\beta u_h, \nabla u_h)_{\Omega_e} = -\langle \beta \cdot n_{\partial\Omega}, \frac{1}{2} u_h^2 \rangle_{\partial\Omega} - \sum_{F \in F^i \cup F^i_{\mathrm{HP}}} \langle \beta \cdot n_F, \frac{1}{2} [u_h^2] \rangle_F.$$

Thus taking $v_h = u_h$ in (2.8) yields:

$$\begin{aligned} &\frac{1}{2}\frac{d}{dt}\|u_h\|_\Omega^2 + \sum_{\Omega_e \in \mathcal{T}_h} \|\epsilon^{1/2} \nabla u_h\|_{\Omega_e}^2 + \frac{1}{2} \sum_{F \in F^i \cup F^i_{\mathrm{HP}}} \| |\beta \cdot n_F|^{1/2} [u_h] \|_F^2 \\ &+\frac{1}{2} \sum_{F \in F^\partial_{\mathrm{in}} \cup F^\partial_{\mathrm{out}}} \| |\beta \cdot n_F|^{1/2} u_h \|_F^2 + \sum_{F \in F^i} |F|^{-1} \|\sigma_F^{1/2} [u_h]\|_F^2 \\ &-(1-\kappa) \sum_{F \in F^i} \langle \{\epsilon \nabla u_h \cdot n_F\}, [u_h] \rangle_F + d(u_h, u_h) = L(u_h). \end{aligned} \tag{3.12}$$

Using Young's inequality, we bound $L(u_h)$:

$$|L(u_h)| \leq \frac{1}{4} \sum_{F \in F^\partial_{\mathrm{in}}} \| |\beta \cdot n_F|^{1/2} u_h \|_F^2 + \sum_{F \in F^\partial_{\mathrm{in}}} \| |\beta \cdot n_F|^{1/2} u_{\mathrm{in}} \|_F^2 + \frac{1}{4} \|f\|_\Omega^2 + \|u_h\|_\Omega^2,$$

and the equation (3.12) becomes:

$$\begin{aligned} &\frac{1}{2}\frac{d}{dt}\|u_h\|_\Omega^2 + \sum_{\Omega_e \in \mathcal{T}_h} \|\epsilon^{1/2} \nabla u_h\|_{\Omega_e}^2 + \frac{1}{2} \sum_{F \in F^i \cup F^i_{\mathrm{HP}}} \| |\beta \cdot n_F|^{1/2} [u_h] \|_F^2 \\ &+\frac{1}{2} \sum_{F \in F^\partial_{\mathrm{out}}} \| |\beta \cdot n_F|^{1/2} u_h \|_F^2 + \frac{1}{4} \sum_{F \in F^\partial_{\mathrm{in}}} \| |\beta \cdot n_F|^{1/2} u_h \|_F^2 \\ &+ \sum_{F \in F^i} |F|^{-1} \|\sigma_F^{1/2} [u_h]\|_F^2 + d(u_h, u_h) \leq \sum_{F \in F^\partial_{\mathrm{in}}} \| |\beta \cdot n_F|^{1/2} u_{\mathrm{in}} \|_F^2 + \frac{1}{4} \|f\|_\Omega^2 + \|u_h\|_\Omega^2 \\ &+|(1-\kappa) \sum_{F \in F^i_{\mathrm{HP}}} \langle \{\epsilon \nabla u_h \cdot n_F\}, [u_h] \rangle_F|. \end{aligned} \tag{3.13}$$

Let us first assume that $\kappa = 1$ in (2.6). It remains to bound the diffusive flux term $d(u_h, u_h)$. In the case where $\delta = 0$, we have $d_1 = 0$ and $d_2 = j_{\tilde{\sigma}}$. This yields for $k = 1, 2$:

$$\frac{d}{dt}\|u_h\|_\Omega^2 + |||u_h|||_k^2 \leq \sum_{F \in F^\partial_{\mathrm{in}}} \| |\beta \cdot n_F|^{1/2} u_{\mathrm{in}} \|_F^2 + \frac{1}{4} \|f\|_\Omega^2 + \|u_h\|_\Omega^2. \tag{3.14}$$

We now integrate from 0 to T and use Gronwall's lemma to obtain the stability bound. In the case where $\delta > 0$, for $\tilde{\kappa} = 1$, we have

$$d_1 = 0, \quad d_2 = d_3 = j_{\tilde{\sigma}},$$

and (3.14) holds. Thus, the bound is obtained as above. For $\tilde{\kappa} = 0$, we have

$$d_1 = -\delta\nu, \quad d_2 = -\delta\nu + j_{\tilde{\sigma}}, \quad d_3 = -\alpha + j_{\tilde{\sigma}}.$$

We then remark that $\delta\nu(u_h, u_h)$ can be bounded by

$$\begin{aligned}
\delta\nu(u_h,u_h) &= \delta \sum_{F\in F^i_{\mathrm{HP}}} \langle (\epsilon\nabla u_h)^{\uparrow}, [u_h]\rangle_F \\
&\le \delta\sqrt{\epsilon^{\Delta}_H} \sum_{F\in F^i_{\mathrm{HP}}} \|\epsilon_H^{1/2}\nabla u_h|_{\Omega_H}\|_F \|[u_h]\|_F \\
&\le C_\tau\, \delta\sqrt{\epsilon^{\Delta}_H} h^{-1} \|u_h\|_\Omega (\sum_{\Omega_e\in\Delta_H} \|\epsilon^{1/2}\nabla u_h\|^2_{\Omega_e})^{1/2} \\
&\le C_\tau\, \|u_h\|^2_\Omega + \delta^2 \epsilon^{\Delta}_H h^{-2} \sum_{\Omega_e\in\Delta_H} \|\epsilon^{1/2}\nabla u_h\|^2_{\Omega_e}. \qquad (3.15)
\end{aligned}$$

Therefore, for $k=1$, the equation (3.13) becomes

$$\begin{aligned}
&\frac{1}{2}\frac{d}{dt}\|u_h\|^2_\Omega + \sum_{\Omega_e\in\mathcal{T}_h\setminus\Delta_H} \|\epsilon^{1/2}\nabla u_h\|^2_{\Omega_e} + \frac{1}{2}\sum_{F\in F^i\cup F^i_{\mathrm{HP}}} \||\beta\cdot n_F|^{1/2}[u_h]\|^2_F \\
&\quad + \frac{1}{2}\sum_{F\in F^\partial_{\mathrm{out}}} \||\beta\cdot n_F|^{1/2}u_h\|^2_F + \frac{1}{4}\sum_{F\in F^\partial_{\mathrm{in}}} \||\beta\cdot n_F|^{1/2}u_h\|^2_F \\
&\quad + (1-\epsilon^{\Delta}_H\delta^2 h^{-2}) \sum_{\Omega_e\in\Delta_H} \|\epsilon^{1/2}\nabla u_h\|^2_{\Omega_e} + \sum_{F\in F^i} |F|^{-1}\|\sigma_F^{1/2}[u_h]\|^2_F \\
&\quad \le C_\tau\, \|u_h\|^2_\Omega + \sum_{F\in F^\partial_{\mathrm{in}}} \||\beta\cdot n_F|^{1/2}u_{\mathrm{in}}\|^2_F + \frac{1}{4}\|f\|^2_\Omega.
\end{aligned}$$

Under Condition II and using Gronwall's lemma, we obtain the desired result. In the case $k=2$, the diffusive term is $d(u_h,u_h) = -\delta\nu(u_h,u_h) + j_{\tilde\sigma}(u_h,u_h)$ and the term $\delta\nu(u_h,u_h)$ is bounded by using the definition of the jump term:

$$|\delta\nu(u_h,u_h)| \le C_\tau\, \delta^2\epsilon_H \sum_{F\in F^i_{\mathrm{HP}}} |F|^{-1/2}\|[u_h]\|^2_F + \frac{1}{4}\sum_{\Omega_e\in\Delta_H} \|\epsilon^{1/2}\nabla u_h\|^2_{\Omega_e}.$$

Thus, both terms can be hidden in the left-hand side of the equation (3.13) if $\tilde\sigma \ge C_\tau\, \delta^2\epsilon_H$. In other words, we obtain (3.11) if Condition I holds true. Finally, when $k=3$, the following bound is obtained using trace inequality (3.1):

$$\alpha(u_h,u_h) \le \frac{1}{2}\sum_{\Omega_e\in\mathcal{T}_h} \|\epsilon^{1/2}\nabla u_h\|^2_{\Omega_e} + C_{\tau,\epsilon^*} \sum_{F\in F^i_{\mathrm{HP}}} |F|^{-1}\|[u_h]\|^2_F. \qquad (3.16)$$

Thus, (3.13) becomes

$$\begin{aligned}
&\frac{1}{2}\frac{d}{dt}\|u_h\|^2_\Omega + \frac{1}{2}\sum_{\Omega_e\in\mathcal{T}_h} \|\epsilon^{1/2}\nabla u_h\|^2_{\Omega_e} + \frac{1}{2}\sum_{F\in F^i\cup F^i_{\mathrm{HP}}} \||\beta\cdot n_F|^{1/2}[u_h]\|^2_F \\
&\quad + \frac{1}{2}\sum_{F\in F^\partial_{\mathrm{out}}} \||\beta\cdot n_F|^{1/2}u_h\|^2_F + \frac{1}{4}\sum_{F\in F^\partial_{\mathrm{in}}} \||\beta\cdot n_F|^{1/2}u_h\|^2_F \\
&\quad + \sum_{F\in F^i} |F|^{-1}\|\sigma_F^{1/2}[u_h]\|^2_F + (\tilde\sigma - C_{\tau,\epsilon^*}) \sum_{F\in F^i_{\mathrm{HP}}} |F|^{-1}\|[u_h]\|^2_F \\
&\quad \le \sum_{F\in F^\partial_{\mathrm{in}}} \||\beta\cdot n_F|^{1/2}u_{\mathrm{in}}\|^2_F + \|f\|^2_\Omega + \|u_h\|^2_\Omega.
\end{aligned}$$

Then, Condition I, integration from 0 to T and Gronwall's lemma yield the stability bound. Finally, in the case $\tilde{\kappa} = -1$, the diffusive fluxes are:

$$d_1 = -2\delta\nu, \quad d_2 = -2\delta\nu + j_{\tilde{\sigma}}, \quad d_3 = -2\alpha + j_{\tilde{\sigma}}.$$

It is clear that as above, Condition II is needed for $d = d_1$, Condition I is needed for $d = d_2$ and for $d = d_3$. It remains to consider the case $\kappa = -1$. Clearly we obtain the same bound under the condition that σ is bounded below by a large enough constant. □

REMARK 3.3. *Existence and uniqueness of the solution of (2.8) is a corollary of the stability result Theorem 3.2 and the theory of ordinary differential equations.*

We next determine the consistency of the proposed schemes. It is easy to check that the solution u of (2.1) satisfies:

$$\forall v_h \in V_h, \quad (\frac{\partial u}{\partial t}, v_h) + A(u, v_h) + e_c(u, v_h) = L(v_h), \tag{3.17}$$

where $e_c = 0$ for $d = d_3$ and $e_c = -(1-\delta)\nu$ for $d = d_1$ or d_2. Therefore, we have the following result.

THEOREM 3.4. *In (2.8)-(2.9), assume that $a = a_1$. The scheme is consistent if $d = d_3$. If $d = d_1$ or $d = d_2$, the consistency error is:*

$$\forall v_h \in V_h, \quad e_c(u, v_h) = -(1-\delta)\nu(u, v_h),$$

where u is the solution of (2.1)-(2.4).

3.3. Semi-Discrete Error Analysis. We next derive a semi-discrete a priori error estimate in the energy norm. Recall that $u^*(t) \in V_h \cap \mathcal{C}^0(\Omega)$ is a continuous interpolant of u that satisfies approximation properties (3.9)-(3.10).

THEOREM 3.5. *For $t > 0$, let $u_h(t)$ be the semi-discrete solution in V_h to (2.8)-(2.9) and assume that $a = a_1$ and for given $k = 1, 2, 3$, fix $d = d_k$. Assume that $u_0 \in H^{p+1}(\Omega)$, $u \in L^2(0, T; H^{p+1}(\Omega))$ and $\partial_t u \in L^2(0, T; H^p(\Omega))$. Then there exists a constant $C_{i,\tau,t,\beta,a,\sigma,\epsilon^*}$ independent of h, ϵ_*, and δ such that*

$$\|(u - u_h)(T)\|_\Omega^2 + \int_0^T |||u(t) - u_h(t)|||_k^2 dt \leq$$
$$C_{i,\tau,t,\beta,a,\sigma,\epsilon^*}\, h^{2p}\Big(|u_0|^2_{H^{p+1}(\Omega)} + \int_0^T |u(t)|^2_{H^{p+1}(\Omega)} dt + \int_0^T |\partial_t u(t)|^2_{H^p(\Omega)} dt\Big), \tag{3.18}$$

for the following cases:

- $\delta = 1, k = 2, \tilde{\kappa} = 1$. *Note that the constant also depends on $\tilde{\sigma}_0^{-1}$ if $\tilde{\sigma} = \tilde{\sigma}_0$. If $\tilde{\sigma} = 1$ or $\tilde{\sigma} = \epsilon_H$, the constant is independent of $\tilde{\sigma}$.*
- $\delta = 1, k = 2, \tilde{\kappa} \in \{-1, 0\}$, $\tilde{\sigma} = 1$ *and* $\sqrt{\epsilon_H^\Delta}$ *small enough.*
- $\delta = 1, k = 2, \tilde{\kappa} \in \{-1, 0\}$, $\tilde{\sigma} = \tilde{\sigma}_0$ *and Condition I. The constant depends on* $\tilde{\sigma}_0^{-1}$.
- $\delta = 1, k = 2, \tilde{\kappa} \in \{-1, 0\}$, $\tilde{\sigma} = \epsilon_H$ *and Condition II.*
- $k = 3, \tilde{\kappa} = 1, \tilde{\sigma} \in \{1, \tilde{\sigma}_0\}$. *The constant depends on $\tilde{\sigma}_0^{-1}$ if $\tilde{\sigma} = \tilde{\sigma}_0$.*
- $k = 3, \tilde{\kappa} \in \{-1, 0\}$ *and $\tilde{\sigma} = \tilde{\sigma}_0$ and Condition I. The constant depends on $\tilde{\sigma}_0^{-1}$ if $\tilde{\sigma} = \tilde{\sigma}_0$.*

The estimate is

$$\|(u-u_h)(T)\|_\Omega^2+\int_0^T |||u(t)-u_h(t)|||_k^2 dt \leq$$
$$C_{i,\tau,t,\beta,a,\sigma,\epsilon^*}\, h^{2p}\Big(|u_0|^2_{H^{p+1}(\Omega)}+(1+\frac{\epsilon^*}{\min\limits_{x\in\Delta_H}\epsilon_H(x)})\int_0^T |u(t)|^2_{H^{p+1}(\Omega)}dt+\int_0^T |\partial_t u(t)|^2_{H^p(\Omega)}dt\Big) \tag{3.19}$$

for the case

- $k=3, \quad \tilde{\kappa}=1, \quad \tilde{\sigma}=\epsilon_H.$

The estimate is

$$\|(u-u_h)(T)\|_\Omega^2+\int_0^T |||u(t)-u_h(t)|||_k^2 dt \leq$$
$$C_{i,\tau,t,\beta,a,\sigma,\epsilon^*}\, h^{2p}(|u_0|^2_{H^{p+1}(\Omega)}+(1+(\epsilon_H^\Delta h^{-1})^2)\int_0^T |u(t)|^2_{H^{p+1}(\Omega)}dt+\int_0^T |\partial_t u(t)|^2_{H^p(\Omega)}dt) \tag{3.20}$$

for the case:

- $\delta=1, k=1, \tilde{\kappa}\in\{-1,0,1\}$ *under Condition II.*

The estimate is

$$\|(u-u_h)(T)\|_\Omega^2+\int_0^T |||u(t)-u_h(t)|||_k^2 dt \leq C_t(\epsilon_H^\Delta h^{-1})^2\int_0^T \|u\|^2_{H^2(\Omega)}$$
$$+C_{i,\tau,t,\beta,a,\sigma,\epsilon^*}\, h^{2p}\Big(|u_0|^2_{H^{p+1}(\Omega)}+\int_0^T |u(t)|^2_{H^{p+1}(\Omega)}dt+\int_0^T |\partial_t u(t)|^2_{H^p(\Omega)}dt\Big) \tag{3.21}$$

for the cases:

- $\delta=0, k\in\{1,2\}.$
- $0<\delta<1, k=1, \tilde{\kappa}\in\{-1,0\}$ *and Condition II.*
- $0<\delta<1, k=2, \tilde{\kappa}=1.$
- $0<\delta<1, k=2, \tilde{\kappa}\in\{-1,0\}$, $\tilde{\sigma}=1$ *and* $\delta\sqrt{\epsilon_H^\Delta}$ *small enough.*
- $0<\delta<1, k=2, \tilde{\kappa}\in\{-1,0\}$, $\tilde{\sigma}=\tilde{\sigma}_0$ *and Condition I.*
- $0<\delta<1, k=2, \tilde{\kappa}\in\{-1,0\}$, $\tilde{\sigma}=\epsilon_H.$

Finally the estimate is

$$\|(u-u_h)(T)\|_\Omega^2+\int_0^T |||u(t)-u_h(t)|||_k^2 dt \leq C_t((1-\delta)\epsilon_H^\Delta h^{-1})^2\int_0^T \|u\|^2_{H^2(\Omega)}$$
$$+C_{i,\tau,t,\beta,a,\sigma,\epsilon^*}\, h^{2p}\Big(|u_0|^2_{H^{p+1}(\Omega)}+(1+\delta^2(\epsilon_H^\Delta h^{-1})^2)\int_0^T |u(t)|^2_{H^{p+1}(\Omega)}dt+\int_0^T |\partial_t u(t)|^2_{H^p(\Omega)}dt\Big) \tag{3.22}$$

for the case

- $0<\delta<1, k=1$ *and* $\tilde{\kappa}=1.$

Proof. Subtracting (3.17) from (2.8) gives the error equation:

$$
\begin{aligned}
&(\partial_t(u_h-u),v_h)_\Omega-\sum_{\Omega_e\in\mathcal{T}_h}(\beta(u_h-u)-\epsilon\nabla(u_h-u),\nabla v_h)_{\Omega_e}\\
&+\sum_{F\in F^i\cup F^i_{\rm HP}}\langle\beta(u_h-u)^\uparrow\cdot n_F,[v_h]\rangle_F-\sum_{F\in F^i}\langle\{\epsilon\nabla(u_h-u)\cdot n_F\},[v_h]\rangle_F\\
&+\kappa\sum_{F\in F^i}\langle\{\epsilon\nabla v_h\cdot n_F\},[u_h-u]\rangle_F+\sum_{F\in F^i}|F|^{-1}\langle\sigma_F[u_h-u],[v_h]\rangle_F\\
&+\sum_{F\in F^\partial_{\rm out}}\langle\beta(u_h-u),v_h\rangle_F+d(u_h-u,v_h)=e_c(u,v_h).
\end{aligned}
\tag{3.23}
$$

We decompose the error $u_h-u=\eta-\xi$ with $\eta=u_h-u^*$ and $\xi=u-u^*$, with u^* satisfying (3.9)-(3.10). Then, choosing $v_h=\eta$ in the error equation (3.23) yields:

$$
\begin{aligned}
&\frac{1}{2}\frac{d}{dt}\|\eta\|^2_\Omega+\sum_{\Omega_e\in\mathcal{T}_h}\|\epsilon^{1/2}\nabla\eta\|^2_{\Omega_e}+\sum_{F\in F^i}|F|^{-1}\|\sigma_F^{1/2}[\eta]\|^2_F\\
&+\frac{1}{2}\sum_{F\in F^i\cup F^i_{\rm HP}}\||\beta\cdot n_F|^{1/2}[\eta]\|^2_F+\frac{1}{2}\sum_{F\in F^\partial_{\rm in}\cup F^\partial_{\rm out}}\||\beta\cdot n_F|^{1/2}\eta\|^2_F\\
&=(\partial_t\xi,\eta)_\Omega-\sum_{\Omega_e\in\mathcal{T}_h}(\beta\xi,\nabla\eta)_{\Omega_e}+\sum_{\Omega_e\in\mathcal{T}_h}(\epsilon\nabla\xi,\nabla\eta)_{\Omega_e}+\sum_{F\in F^i\cup F^i_{\rm HP}}\langle\beta\xi^\uparrow\cdot n_F,[\eta]\rangle_F\\
&-\sum_{F\in F^i}\langle\{\epsilon\nabla\xi\cdot n_F\},[\eta]\rangle_F+\kappa\sum_{F\in F^i}\langle\{\epsilon\nabla\eta\cdot n_F\},[\xi]\rangle_F+\sum_{F\in F^i}|F|^{-1}\langle\sigma_F[\xi],[\eta]\rangle_F\\
&+\sum_{F\in F^\partial_{\rm out}}\langle\beta\xi\cdot n_F,\eta\rangle_F-(1-\kappa)\sum_{F\in F^i}\langle\{\epsilon\nabla\eta\cdot n_F\},[\eta]\rangle_F+e_c(u,\eta)+d(\xi,\eta)-d(\eta,\eta)\\
&=T_1+\cdots+T_{12}.
\end{aligned}
\tag{3.24}
$$

We now briefly bound the first nine terms. The techniques used are standard to the discontinuous Galerkin methods. The first term T_1 is easily bounded by Cauchy-Schwarz and Young's inequalities:

$$
T_1\le\frac{1}{2}\|\eta\|^2_\Omega+\frac{1}{2}\|\partial_t\xi\|^2_\Omega.
$$

Using inverse inequality (3.8), the second term is bounded as

$$
\begin{aligned}
T_2&\le\|\beta\|_\infty\|\xi\|_\Omega(\sum_{\Omega_e\in\mathcal{T}_h}\|\nabla\eta\|^2_{\Omega_e})^{1/2}\\
&\le C_ih^{-1}\|\beta\|_\infty\|\xi\|_\Omega(\sum_{\Omega_e\in\mathcal{T}_h}\|\eta\|^2_{\Omega_e})^{1/2}\\
&\le\frac{1}{2}\|\eta\|^2_\Omega+C_ih^{-2}\frac{1}{2}\|\beta\|^2_\infty\|\xi\|^2_\Omega.
\end{aligned}
\tag{3.25}
$$

Similarly the term T_3 is bounded

$$
\begin{aligned}
T_3&\le\sqrt{\epsilon^*}\sum_{\Omega_e\in\mathcal{T}_h}\|\epsilon^{1/2}\nabla\eta\|_{\Omega_e}\|\nabla\xi\|_{\Omega_e}\\
&\le\frac{1}{16}\sum_{\Omega_e\in\mathcal{T}_h}\|\epsilon^{1/2}\nabla\eta\|^2_{\Omega_e}+4\epsilon^*\|\nabla\xi\|^2_\Omega.
\end{aligned}
\tag{3.26}
$$

For the fourth term we have:

$$T_4 \leq \|\beta\|_\infty^{1/2} \sum_{F\in F^i\cup F^i_{\mathrm{HP}}} \|\xi^\uparrow\|_F \||\beta\cdot n_F|^{1/2}[\eta]\|_F$$
$$\leq \frac{1}{16}\sum_{F\in F^i\cup F^i_{\mathrm{HP}}} \||\beta\cdot n_F|^{1/2}[\eta]\|_F^2 + 4\|\beta\|_\infty \sum_{F\in F^i\cup F^i_{\mathrm{HP}}} \|\xi^\uparrow\|_F^2. \tag{3.27}$$

We have for T_5:

$$T_5 \leq \frac{1}{16}\sum_{F\in F^i} |F|^{-1}\|\sigma_F^{1/2}[\eta]\|_F^2 + \epsilon^* h \sum_{F\in F^i}\sigma_F^{-1}\|\{\nabla\xi\cdot n_F\}\|_F^2. \tag{3.28}$$

By continuity of ξ, the term T_6 vanishes. The term T_7 is easily bounded

$$T_7 \leq \frac{1}{16}\sum_{F\in F^i} |F|^{-1}\|\sigma_F^{1/2}[\eta]\|_F^2 + 4\sum_{F\in F^i}|F|^{-1}\|\sigma_F^{1/2}[\xi]\|_F^2. \tag{3.29}$$

The term T_8 is bounded similar to T_4,

$$T_8 \leq \frac{1}{16}\sum_{F\in F^\partial_{\mathrm{out}}} \||\beta\cdot n_F|^{1/2}\eta\|_F^2 + 4\|\beta\|_\infty\sum_{F\in F^\partial_{\mathrm{out}}}\|\xi\|_F^2.$$

If $\kappa = 1$, the term T_9 vanishes. Otherwise, we use a similar argument as in (3.16) using (3.1):

$$T_9 \leq \frac{1}{8}\sum_{\Omega_e\in\mathcal{T}_h}\|\epsilon^{1/2}\nabla\eta\|_{\Omega_e}^2 + C_{\tau,\epsilon^*}\sum_{F\in F^i_{\mathrm{HP}}}|F|^{-1}\|[\eta]\|_F^2. \tag{3.30}$$

Combining the bounds above, for $\kappa = 1$, equation (3.24) becomes:

$$\frac{1}{2}\frac{d}{dt}\|\eta\|_\Omega^2 + \frac{3}{4}\sum_{\Omega_e\in\mathcal{T}_h}\|\epsilon^{1/2}\nabla\eta\|_{\Omega_e}^2 + \frac{7}{8}\sum_{F\in F^i}|F|^{-1}\|\sigma_F^{1/2}[\eta]\|_F^2$$
$$+\frac{7}{16}\sum_{F\in F^i\cup F^i_{\mathrm{HP}}}\||\beta\cdot n_F|^{1/2}[\eta]\|_F^2 + \frac{1}{2}\sum_{F\in F^\partial_{\mathrm{in}}}\||\beta\cdot n_F|^{1/2}\eta\|_F^2 + \frac{7}{16}\sum_{F\in F^\partial_{\mathrm{out}}}\||\beta\cdot n_F|^{1/2}\eta\|_F^2$$
$$\leq \|\eta\|_\Omega^2 + \frac{1}{2}\|\partial_t\xi\|_\Omega^2 + C_i h^{-2}\|\beta\|_\infty^2\|\xi\|_\Omega^2 + 4\epsilon^*\|\nabla\xi\|_\Omega^2 + 4\sum_{F\in F^i}|F|^{-1}\|\sigma_F^{1/2}[\xi]\|_F^2$$
$$+4\|\beta\|_\infty\sum_{F\in F^i\cup F^i_{\mathrm{HP}}}\|\xi^\uparrow\|_F^2 + \epsilon^* h\sum_{F\in F^i}\sigma_F^{-1}\|\{\nabla\xi\cdot n_F\}\|_F^2 + 4\|\beta\|_\infty\sum_{F\in F^\partial_{\mathrm{out}}}\|\xi\|_F^2$$
$$+e_c(u,\eta) + d(\xi,\eta) - d(\eta,\eta)$$
$$\leq \|\eta\|_\Omega^2 + C_{i,\tau,t,\beta,a,\sigma,\epsilon^*}\,h^{2p}(|u|_{H^{p+1}(\Omega)}^2 + |\partial_t u|_{H^p(\Omega)}^2) + e_c(u,\eta) + d(\xi,\eta) - d(\eta,\eta). \tag{3.31}$$

If $\kappa = -1$, the resulting equation differs from (3.31) only by the constant in front of $\sum_{F\in F^i}|F|^{-1}\|\sigma_F^{1/2}[\eta]\|_F^2$. We will now continue the analysis of the scheme by considering each diffusive flux separately.

Case: $d = d_1$: If $\delta = 0$, the last three terms reduce to the consistency error only

$$T_{10} + T_{11} + T_{12} = -\nu(u,\eta)$$
$$\leq C_t\epsilon_H^\Delta h^{-1}\|\eta\|_\Omega\|u\|_{H^2(\Omega)}$$
$$\leq \frac{1}{2}\|\eta\|_\Omega^2 + C_t(\epsilon_H^\Delta h^{-1})^2\|u\|_{H^2(\Omega)}^2. \tag{3.32}$$

Therefore, integrating (3.31) from 0 to t and using Gronwall's lemma gives:

$$\|\eta(t)\|_\Omega^2 + \int_0^t |||\eta|||_1^2 \le \|\eta(0)\|_\Omega^2 + C_{i,\tau,t,\beta,a,\sigma,\epsilon^*}\, h^{2p} \int_0^t (|u|_{H^{p+1}(\Omega)}^2 + |\partial_t u|_{H^p(\Omega)}^2) \\ + C_t(\epsilon_H^\Delta h^{-1})^2 \int_0^t \|u\|_{H^2(\Omega)}^2. \tag{3.33}$$

Therefore, for $d = d_1$ and $\delta = 0$, we have optimal bounds if $\epsilon_H^\Delta \le h^{p+1}$ and if we assume that $u \in L^2(0,T;H^2(\Omega))$. Let us now consider $0 < \delta < 1$. The consistency error is bounded similarly as in (3.32):

$$T_{10} \le \frac{1}{2}\|\eta\|_\Omega^2 + C_t(1-\delta)^2(\epsilon_H^\Delta h^{-1})^2 \|u\|_{H^2(\Omega)}^2. \tag{3.34}$$

By continuity of ξ and by the approximation result (3.9), we have

$$T_{11} = -\delta\nu(\xi,\eta) \le \frac{1}{2}\|\eta\|_\Omega^2 + C_{\tau,t,a}\, \delta^2(\epsilon_H^\Delta h^{-1})^2 h^{2p} |u|_{H^{p+1}(\Omega)}^2. \tag{3.35}$$

Now if $\tilde\kappa = 1$, the last term T_{12} vanishes and the error equation (3.31) with (3.34), (3.35) and Gronwall's lemma becomes

$$\|\eta(t)\|_\Omega^2 + \int_0^t |||\eta|||_1^2 \le C_{i,\tau,t,\beta,a,\sigma,\epsilon^*}\, h^{2p}((1+\delta^2(\epsilon_H^\Delta h^{-1})^2)) \int_0^t |u|_{H^{p+1}(\Omega)}^2 + \int_0^t |\partial_t u|_{H^p(\Omega)}^2) \\ + C_t(1-\delta)^2(\epsilon_H^\Delta h^{-1})^2 \int_0^t \|u\|_{H^2(\Omega)}^2 + \|\eta(0)\|_\Omega^2. \tag{3.36}$$

This means that optimal bounds are obtained if $\epsilon_H^\Delta \le h^{p+1}$. If $\tilde\kappa \in \{-1, 0\}$, we have from (3.15):

$$T_{12} = (1-\tilde\kappa)\nu(\eta,\eta) \le C_\tau \|\eta\|_\Omega^2 + \delta^2 \epsilon_H^\Delta h^{-2} \sum_{\Omega_e \in \Delta_H} \|\epsilon^{1/2}\nabla\eta\|_{\Omega_e}^2. \tag{3.37}$$

Therefore, using Condition II and (3.34), (3.35), we obtain:

$$\|\eta(t)\|_\Omega^2 + \int_0^t |||\eta|||_1^2 \le \|\eta(0)\|_\Omega^2 + C_{i,\tau,t,\beta,a,\sigma,\epsilon^*}\, h^{2p}\Big(\int_0^t |u|_{H^{p+1}(\Omega)}^2 + \int_0^t |\partial_t u|_{H^p(\Omega)}^2\Big) \\ + C_t(1-\delta)^2(\epsilon_H^\Delta h^{-1})^2 \int_0^t \|u\|_{H^2(\Omega)}^2. \tag{3.38}$$

Finally, if $\delta = 1$, the consistency error vanishes. In the case $\tilde\kappa = 1$, the terms T_{10}, T_{12} vanish and we use (3.35) to bound T_{11}. The error estimate is optimal if $\epsilon_H^\Delta \le h$:

$$\|\eta(t)\|_\Omega^2 + \int_0^t |||\eta|||_k^2 \le \|\eta(0)\|_\Omega^2 \\ + C_{i,\tau,t,\beta,a,\sigma,\epsilon^*}\, h^{2p}\Big((1+(\epsilon_H^\Delta h^{-1})^2) \int_0^t |u|_{H^{p+1}(\Omega)}^2 + \int_0^t |\partial_t u|_{H^p(\Omega)}^2\Big). \tag{3.39}$$

If $\tilde\kappa \in \{-1, 0\}$ and $\delta = 1$, we obtain (3.37) and have (3.39) by Condition II.

Case $d = d_2$: Next, we consider the second numerical flux $d = d_2$. If $\delta = 0$, the last three terms of (3.31) are reduced to $-\nu(u,\eta) + j_{\tilde\sigma}(\xi,\eta) - j_{\tilde\sigma}(\eta,\eta)$. Using (3.32),

the error estimate is the same as (3.33). Let us now fix $0 < \delta < 1$. The case $\tilde{\kappa} = 1$ is handled as before: the term T_{12} vanishes, the term $T_{10} = -(1-\delta)\nu(u,\eta)$ is bounded as (3.34) and the term T_{11} is bounded like (3.35) with a constant depending on $\tilde{\sigma}$ if $\tilde{\sigma} = \tilde{\sigma}_0$. The resulting estimate is (3.36). For $\tilde{\kappa} \in \{-1, 0\}$, we need to bound the additional term $\delta\nu(\eta,\eta)$ corresponding to T_{12}. First, if $\tilde{\sigma} = \tilde{\sigma}_0$ we have:

$$\delta \sum_{F \in F^i_{\mathrm{HP}}} \langle (\epsilon \nabla \eta)^{\uparrow} \cdot n_F, [\eta] \rangle_F \leq \frac{1}{32} \sum_{\Omega_e \in \Delta_H} \|\epsilon^{1/2} \nabla \eta\|^2_{\Omega_e} + C_\tau \delta^2 \epsilon_H^{\Delta} \sum_{F \in F^i_{\mathrm{HP}}} |F|^{-1} \|[\eta]\|^2_F. \tag{3.40}$$

Provided $\tilde{\sigma}_0$ is large enough, both terms can be hidden in the left-hand side of (3.31). The estimate is then (3.33). If $\tilde{\sigma} = 1$, we have

$$\delta \sum_{F \in F^i_{\mathrm{HP}}} \langle (\epsilon \nabla \eta)^{\uparrow} \cdot n_F, [\eta] \rangle_F \leq \frac{1}{32} \sum_{\Omega_e \in \Delta_H} \|\epsilon^{1/2} \nabla \eta\|^2_{\Omega_e} + C_\tau \delta^2 \epsilon_H^{\Delta} j_{\tilde{\sigma}}(\eta,\eta).$$

Both terms can be hidden in the left-hand side of (3.31) if $C_\tau \delta^2 \epsilon_H^{\Delta} < 1$. The estimate is still (3.33). Finally if $\tilde{\sigma} = \epsilon_H$, the bound (3.37) will yield (3.33) under Condition II. Let us assume now that $\delta = 1$ and consider $\tilde{\kappa} = 1$. The consistency error T_{10} vanishes and we are left with

$$T_{11} + T_{12} = -\nu(\xi,\eta) - j_{\tilde{\sigma}}(\eta,\eta).$$

The first term is bounded as follows:

$$-\nu(\xi,\eta) \leq C_{t,a,\epsilon^*}\, h^{2p} |u|^2_{H^{p+1}(\Omega)} + \frac{1}{16} j_{\tilde{\sigma}}(\eta,\eta), \quad \text{if} \quad \tilde{\sigma} = 1, \epsilon_H,$$

or as follows:

$$-\nu(\xi,\eta) \leq C_{t,a,\epsilon^*,\tilde{\sigma}^{-1}}\, h^{2p} |u|^2_{H^{p+1}(\Omega)} + \frac{1}{16} j_{\tilde{\sigma}}(\eta,\eta), \quad \text{if} \quad \tilde{\sigma} = \tilde{\sigma}_0,$$

and the second term can be hidden in the left-hand side of (3.31). Thus, we obtain the estimate:

$$\|\eta(t)\|^2_{\Omega} + \int_0^t |||\eta|||^2_k \leq \|\eta(0)\|^2_{\Omega} + C_{i,\tau,\beta,\epsilon^*,a}\, h^{2p} \Big(\int_0^t |u|^2_{H^{p+1}(\Omega)} + \int_0^t |\partial_t u|^2_{H^p(\Omega)} \Big), \tag{3.41}$$

with the constant depending on $\tilde{\sigma}^{-1}$ if $\tilde{\sigma} = \tilde{\sigma}_0$. If $\delta = 1$ and $\tilde{\kappa} \in \{-1, 0\}$, we need to bound the additional term $-\nu(\eta,\eta)$. Using the same arguments as for $d = d_2$ and $0 < \delta < 1$, we can easily conclude that (3.41) holds if ϵ_H^{Δ} is small enough for $\tilde{\sigma} = 1$; if Condition II holds for $\tilde{\sigma} = \epsilon_H$; and if Condition I holds for $\tilde{\sigma} = \tilde{\sigma}_0$.

Case $d = d_3$: Finally, if $d = d_3$, there is no consistency error and the last three terms in (3.31) are:

$$T_{10} + T_{11} + T_{12} = -\alpha(\xi,\eta) + (1 - \tilde{\kappa})\alpha(\eta,\eta) - j_{\tilde{\sigma}}(\eta,\eta).$$

If $\tilde{\kappa} = 1$ and $\tilde{\sigma} \in \{1, \tilde{\sigma}_0\}$, then we easily obtain the estimate (3.41) using the bound:

$$\alpha(\xi,\eta) \leq C_{t,\tilde{\sigma},\epsilon^*,a}\, h^{2p} |u|^2_{H^{p+1}(\Omega)} + \frac{1}{32} \sum_{F \in F^i_{\mathrm{HP}}} |F|^{-1} \|\tilde{\sigma}^{1/2}[\eta]\|^2_F. \tag{3.42}$$

If $\tilde{\sigma} = \epsilon_H$, then we have

$$\alpha(\xi,\eta) \leq \frac{1}{32} j_{\tilde{\sigma}}(\eta,\eta) + C_{t,a} \frac{\epsilon^*}{\min_{x\in\Delta_H} \epsilon(x)} h^{2p} |u|^2_{H^{p+1}(\Omega)}, \tag{3.43}$$

which yields the estimate (3.19). Finally, the additional term to bound in the case $\tilde{\kappa} \in \{-1, 0\}$ is

$$\alpha(\eta,\eta) \leq \frac{1}{32} \sum_{\Omega_e\in\mathcal{T}_h} \|\epsilon^{1/2}\nabla\eta\|^2_F + C_{\tau,\epsilon^*} \sum_{F\in F^i_{\mathrm{HP}}} |F|^{-1} \|[\eta]\|^2_F, \tag{3.44}$$

which can be subtracted from the left-hand side of (3.31) if $\tilde{\sigma}_0$ is large enough. ∎

A simple corollary of Theorem 3.5 is the convergence of the method in particular cases.

LEMMA 3.6. *Let u_h be solution of (2.8) with $a = a_1$. Assume that the diffusive flux is one of the following*

- $d(u_h, v_h) = -\nu(u_h, v_h) + \nu(v_h, u_h) + j_{\tilde{\sigma}}(u_h, v_h)$
- $d(u_h, v_h) = -\nu(u_h, v_h) - \nu(v_h, u_h) + j_{\tilde{\sigma}}(u_h, v_h)$ *with* $\tilde{\sigma} = \tilde{\sigma}_0$ *large enough.*
- $d(u_h, v_h) = -\nu(u_h, v_h) + j_{\tilde{\sigma}}(u_h, v_h)$ *with* $\tilde{\sigma} = \tilde{\sigma}_0$ *large enough.*
- $d = -\alpha(u_h, v_h) + \alpha(v_h, u_h) + j_{\tilde{\sigma}}(u_h, v_h)$ *with* $\tilde{\sigma} = 1$.
- $d = -\alpha(u_h, v_h) - \alpha(v_h, u_h) + j_{\tilde{\sigma}}(u_h, v_h)$ *with* $\tilde{\sigma} = \tilde{\sigma}_0$ *large enough.*
- $d = -\alpha(u_h, v_h) + j_{\tilde{\sigma}}(u_h, v_h)$ *with* $\tilde{\sigma} = \tilde{\sigma}_0$ *large enough.*

Then, the numerical error converges to zero with optimal convergence rate:

$$\|(u - u_h)(T)\|^2_\Omega + \int_0^T |||u(t) - u_h(t)|||^2_k dt = \mathcal{O}(h^{2p}).$$

We now conclude this section with a few remarks.

REMARK 3.7. *The case $d = 0$ in Fig. 2.2(b) can yield an accurate solution on a given mesh if $\epsilon^\Delta_H \leq h^{p+1}$, but this method does not converge as the mesh size tends to zero.*

REMARK 3.8. *In general, the analysis is valid for degenerate $\epsilon_H = 0$, except in the case $k = 3, \tilde{\kappa} = 1$ and $\tilde{\sigma} = \epsilon_H$. In addition no assumption on the relative size of ϵ_H with respect to ϵ_P is made.*

REMARK 3.9. *Error estimates cannot be obtained for the case $d = d_3$, $\tilde{\kappa} \in \{-1, 0\}$ and $\tilde{\sigma} \in \{1, \epsilon_H\}$.*

4. Fully Discrete Scheme and Analysis. Let Δt be a positive time step and let $t^j = j\Delta t$ denote the time at the j^{th} step. We denote by v^j the function v evaluated at time t^j. We define the linear form $L^{j+1} : V_h \to \mathbb{R}$:

$$L^{j+1}(v_h) = (f^{j+1}, v_h)_\Omega - \sum_{F\in F^\partial_{\mathrm{in}}} \langle \beta u^{j+1}_{\mathrm{in}} \cdot n_F, v_h\rangle_F. \tag{4.1}$$

4.1. Backward Euler time discretization. In this paper, we refer to the implicit DG solution as the solution defined by:

$$\forall v_h \in V_h, \quad (\frac{u^{j+1}_h - u^j_h}{\Delta t}, v_h) + A(u^{j+1}_h, v_h) = L^{j+1}(v_h), \tag{4.2}$$

$$\forall v_h \in V_h, \quad (u^0_h, v_h) = (u_0, v_h). \tag{4.3}$$

We first derive a stability bound then present an error estimate:

THEOREM 4.1. *For $t > 0$, let $(u_h^j)_j$ be the discrete solution in V_h to (4.2)-(4.3) and assume that $a = a_1$ and for given $k = 1, 2, 3$, fix $d = d_k$. If $k = 3$ and $\tilde{\kappa} \in \{-1, 0\}$, assume that Condition I holds true. If $k = 1$, $\delta \neq 0$ and $\tilde{\kappa} \in \{-1, 0\}$, assume that Condition II holds true. Assume that Condition I holds true for $k = 2, \delta \neq 0$ and $\tilde{\kappa} \in \{-1, 0\}$. Then, there is $\Delta t_0 > 0$ such that for all $\Delta t \leq \Delta t_0$, $(u_h^j)_j$ satisfies the bound for all $n > 0$:*

$$\|u_h^n\|_\Omega^2 + C\Delta t \sum_{j=1}^{n} |||u_h^j|||_k^2 dt \leq \|u_0\|_\Omega^2 + C_{\tau,\epsilon^*}\Delta t \sum_{j=1}^{n} (\|f^j\|_\Omega^2 + \sum_{F \in F_{\text{in}}^\partial} \||\beta \cdot n_F|^{1/2} u_{\text{in}}^j\|_F^2). \tag{4.4}$$

where C_{τ,ϵ^*} is a constant independent of $h, \Delta t$ and ϵ_* but depending on C_τ and ϵ^*.

Proof. Choose $v_h = u_h^{j+1}$ in (4.2). We obtain a similar bound as in (3.13):

$$\begin{aligned}
&\frac{1}{2\Delta t}(\|u_h^{j+1}\|_\Omega^2 - \|u_h^j\|_\Omega^2) + \sum_{\Omega_e \in \mathcal{T}_h} \|\epsilon^{1/2}\nabla u_h^{j+1}\|_{\Omega_e}^2 + \frac{1}{2}\sum_{F \in F^i \cup F_{\text{HP}}^i} \||\beta \cdot n_F|^{1/2}[u_h^{j+1}]\|_F^2 \\
&\quad + \frac{1}{2}\sum_{F \in F_{\text{out}}^\partial} \||\beta \cdot n_F|^{1/2} u_h^{j+1}\|_F^2 + \frac{1}{4}\sum_{F \in F_{\text{in}}^\partial} \||\beta \cdot n_F|^{1/2} u_h^{j+1}\|_F^2 \\
&+ \sum_{F \in F^i} |F|^{-1}\|\sigma_F^{1/2}[u_h^{j+1}]\|_F^2 + d(u_h^{j+1}, u_h^{j+1}) \leq \sum_{F \in F_{\text{in}}^\partial} \||\beta \cdot n_F|^{1/2} u_{\text{in}}^{j+1}\|_F^2 + \frac{1}{4}\|f^{j+1}\|_\Omega^2 \\
&\quad + \|u_h^{j+1}\|_\Omega^2 + |(1-\kappa)\sum_{F \in F_{\text{HP}}^i} \langle\{\epsilon\nabla u_h^{j+1} \cdot n_F\}, [u_h^{j+1}]\rangle_F|.
\end{aligned} \tag{4.5}$$

Using similar arguments as in the proof of Theorem 3.2, we obtain:

$$\begin{aligned}
&\frac{1}{2\Delta t}(\|u_h^{j+1}\|_\Omega^2 - \|u_h^j\|_\Omega^2) + C|||u_h^{j+1}|||_k^2 \\
&\leq C_\tau \|u_h^{j+1}\|_\Omega^2 + C_{\tau,\epsilon^*}(\sum_{F \in F_{\text{in}}^\partial} \||\beta \cdot n_F|^{1/2} u_{\text{in}}^{j+1}\|_F^2 + \|f^{j+1}\|_\Omega^2),
\end{aligned} \tag{4.6}$$

We then multiply the inequality by $2\Delta t$ and sum over $j = 0, \ldots, n-1$:

$$\begin{aligned}
&(1 - 2C_\tau\Delta t)\|u_h^n\|_\Omega^2 - \|u_h^0\|_\Omega^2 + 2C\Delta t \sum_{j=1}^{n} |||u_h^j|||_k^2 \\
&\leq 2C_\tau\Delta t \sum_{j=1}^{n-1} \|u_h^j\|_\Omega^2 + 2C_{\tau,\epsilon^*}\Delta t \sum_{j=1}^{n}(\sum_{F \in F_{\text{in}}^\partial} \||\beta \cdot n_F|^{1/2} u_{\text{in}}^j\|_F^2 + \|f^j\|_\Omega^2)
\end{aligned}$$

Under the assumption that $1 - 2C_\tau\Delta t > 0$ and using a discrete Gronwall's estimate, we obtain the final result. ∎

We then remark that the exact solution u satisfies:

$$\forall v_h \in V_h, \quad (\frac{\partial u}{\partial t}(t^{j+1}), v_h) + A(u^{j+1}, v_h) + e_c(u^{j+1}, v_h) = L^{j+1}(v_h), \tag{4.7}$$

where e_c is the consistency error defined in Theorem 3.4.

THEOREM 4.2. *Let u be the solution of (2.1)-(2.4) and let $(u_h^j)_j \in V_h$ be the sequence of discrete solutions satisfying (4.2)-(4.3). Assume that $a = a_1$ and for*

given $k = 1, 2, 3$, fix $d = d_k$. Assume that $u_0 \in H^{p+1}(\Omega)$, $u \in L^2(0,T;H^{p+1}(\Omega))$ and $\partial_t u \in L^2(0,T;H^p(\Omega))$. There is a constant $\Delta t_0 > 0$ such that for all $\Delta t < \Delta t_0$, and constants $C, C_{i,\tau,t,\beta,a,\sigma,\epsilon^*}$ independent of h, ϵ_*, and δ such that

$$\|u^n - u_h^n\|_\Omega^2 + \Delta t \sum_{j=1}^n |||u^j - u_h^j|||_k^2 \leq C\Delta t^2 \int_0^T \|\partial_{tt} u(t)\|_\Omega^2 dt$$

$$+C_{i,\tau,t,\beta,a,\sigma,\epsilon^*}\, h^{2p}\Big(|u_0|^2_{H^{p+1}(\Omega)} + \Delta t \sum_{j=1}^n |u^j|^2_{H^{p+1}(\Omega)} + \Delta t \sum_{j=1}^n |\partial_t u^j|^2_{H^p(\Omega)}\Big), \quad (4.8)$$

for the following cases:

- $\delta = 1, k = 2, \tilde{\kappa} = 1$. *The constant also depends on $\tilde{\sigma}^{-1}$ if $\tilde{\sigma} = \tilde{\sigma}_0$.*
- $\delta = 1, k = 2, \tilde{\kappa} \in \{-1, 0\}$, $\tilde{\sigma} = 1$ *and* $\sqrt{\epsilon_H^\Delta}$ *small enough.*
- $\delta = 1, k = 2, \tilde{\kappa} \in \{-1, 0\}$, $\tilde{\sigma} = \tilde{\sigma}_0$ *and Condition I.*
- $\delta = 1, k = 2, \tilde{\kappa} \in \{-1, 0\}$, $\tilde{\sigma} = \epsilon_H$ *and Condition II.*
- $k = 3, \tilde{\kappa} = 1, \tilde{\sigma} \in \{1, \tilde{\sigma}_0\}$. *The constant also depends on $\tilde{\sigma}^{-1}$ if $\tilde{\sigma} = \tilde{\sigma}_0$.*
- $k = 3, \tilde{\kappa} \in \{-1, 0\}$ *and $\tilde{\sigma} = \tilde{\sigma}_0$ and Condition I. The constant also depends on $\tilde{\sigma}^{-1}$ if $\tilde{\sigma} = \tilde{\sigma}_0$.*

The estimate is

$$\|u^n - u_h^n\|_\Omega^2 + \Delta t \sum_{j=1}^n |||u^j - u_h^j|||_k^2 \leq C\Delta t^2 \int_0^T \|\partial_{tt} u(t)\|_\Omega^2 dt$$

$$+C_{i,\tau,t,\beta,a,\sigma,\epsilon^*}\, h^{2p}\Big(|u_0|^2_{H^{p+1}(\Omega)} + (1 + \frac{\epsilon^*}{\min\limits_{x\in\Delta_H} \epsilon_H(x)}) \int_0^T |u(t)|^2_{H^{p+1}(\Omega)} dt + \int_0^T |\partial_t u(t)|^2_{H^p(\Omega)} dt\Big), \quad (4.9)$$

for the case $k = 3, \quad \tilde{\kappa} = 1, \quad \tilde{\sigma} = \epsilon_H$.
The estimate is

$$\|u^n - u_h^n\|_\Omega^2 + \Delta t \sum_{j=1}^n |||u^j - u_h^j|||_k^2 \leq C\Delta t^2 \int_0^T \|\partial_{tt} u(t)\|_\Omega^2 dt$$

$$+C_{i,\tau,t,\beta,a,\sigma,\epsilon^*}\, h^{2p}\Big(|u_0|^2_{H^{p+1}(\Omega)} + (1 + (\epsilon_H^\Delta h^{-1})^2) \int_0^T |u(t)|^2_{H^{p+1}(\Omega)} dt + \int_0^T |\partial_t u(t)|^2_{H^p(\Omega)} dt\Big), \quad (4.10)$$

for the case $\delta = 1, k = 1, \tilde{\kappa} \in \{-1, 0, 1\}$ under Condition II.
The estimate is

$$\|u^n - u_h^n\|_\Omega^2 + \Delta t \sum_{j=1}^n |||u^j - u_h^j|||_k^2 \leq C_t(\epsilon_H^\Delta h^{-1})^2 \int_0^T \|u\|^2_{H^2(\Omega)} + C\Delta t^2 \int_0^T \|\partial_{tt} u(t)\|_\Omega^2 dt$$

$$+C_{i,\tau,t,\beta,a,\sigma,\epsilon^*}\, h^{2p}\Big(|u_0|^2_{H^{p+1}(\Omega)} + \int_0^T |u(t)|^2_{H^{p+1}(\Omega)} dt + \int_0^T |\partial_t u(t)|^2_{H^p(\Omega)} dt\Big), \quad (4.11)$$

for the cases:

- $\delta = 0, k \in \{1, 2\}$.
- $0 < \delta < 1, k = 1, \tilde{\kappa} \in \{-1, 0\}$ *and Condition II.*
- $0 < \delta < 1, k = 2, \tilde{\kappa} = 1$.

- $0 < \delta < 1, k = 2, \tilde{\kappa} \in \{-1, 0\}$, $\tilde{\sigma} = 1$ *and* $\delta\sqrt{\epsilon_H^{\Delta}}$ *small enough.*
- $0 < \delta < 1, k = 2, \tilde{\kappa} \in \{-1, 0\}$, $\tilde{\sigma} = \tilde{\sigma}_0$ *and Condition I.*
- $0 < \delta < 1, k = 2, \tilde{\kappa} \in \{-1, 0\}$, $\tilde{\sigma} = \epsilon_H$.

Finally the estimate is

$$\|u^n - u_h^n\|_{\Omega}^2 + \Delta t \sum_{j=1}^{n} |||u^j - u_h^j|||_k^2 \leq C_t((1-\delta)\epsilon_H^{\Delta} h^{-1})^2 \int_0^T \|u\|_{H^2(\Omega)}^2 + C\Delta t^2 \int_0^T \|\partial_{tt} u(t)\|_{\Omega}^2 dt$$
$$+C_{i,\tau,t,\beta,a,\sigma,\epsilon^*} h^{2p} \Big(|u_0|_{H^{p+1}(\Omega)}^2 + (1 + \delta^2(\epsilon_H^{\Delta} h^{-1})^2) \int_0^T |u(t)|_{H^{p+1}(\Omega)}^2 dt + \int_0^T |\partial_t u(t)|_{H^p(\Omega)}^2 dt \Big), \tag{4.12}$$

for the case $0 < \delta < 1, k = 1$ *and* $\tilde{\kappa} = 1$.

Proof. Using the same notation as in the proof of Theorem 3.5, we have from subtracting (4.7) from (4.2):

$$\forall v_h \in V_h, \quad (\frac{\eta^{j+1} - \eta^i}{\Delta t}, v_h)_{\Omega} + A(\eta^{j+1}, v_h) = A(\xi^{j+1}, v_h) + (\partial_t \xi(t^{j+1}), v_h)$$
$$+(\partial_t u^*(t^{j+1}) - \frac{u^{*j+1} - u^{*j}}{\Delta t}, v_h)_{\Omega} + e_c(u^{j+1}, v_h). \tag{4.13}$$

Choosing $v_h = \eta^{j+1}$ yields a similar expression as (3.24)

$$\frac{1}{2\Delta t}(\|\eta^{j+1}\|_{\Omega}^2 - \|\eta^j\|_{\Omega}^2) + \sum_{\Omega_e \in \mathcal{T}_h} \|\epsilon^{1/2} \nabla \eta^{j+1}\|_{\Omega_e}^2 + \sum_{F \in F^i} |F|^{-1} \|\sigma_F^{1/2} [\eta^{j+1}]\|_F^2$$
$$+\frac{1}{2} \sum_{F \in F^i \cup F_{\mathrm{HP}}^i} \||\beta \cdot n_F|^{1/2} [\eta^{j+1}]\|_F^2 + \frac{1}{2} \sum_{F \in F_{\mathrm{in}}^{\partial} \cup F_{\mathrm{out}}^{\partial}} \||\beta \cdot n_F|^{1/2} \eta^{j+1}\|_F^2$$
$$= (\partial_t u^*(t^{j+1}) - \frac{u^{*j+1} - u^{*j}}{\Delta t}, \eta^{j+1})_{\Omega} + (\partial_t \xi(t^{j+1}), \eta^{j+1})_{\Omega} - \sum_{\Omega_e \in \mathcal{T}_h} (\beta \xi^{j+1}, \nabla \eta^{j+1})_{\Omega_e}$$
$$+ \sum_{\Omega_e \in \mathcal{T}_h} (\epsilon \nabla \xi^{j+1}, \nabla \eta^{j+1})_{\Omega_e} + \sum_{F \in F^i \cup F_{\mathrm{HP}}^i} \langle \beta \xi^{\uparrow, j+1} \cdot n_F, [\eta^{j+1}] \rangle_F$$
$$- \sum_{F \in F^i} \langle \{\epsilon \nabla \xi^{j+1} \cdot n_F\}, [\eta^{j+1}] \rangle_F + \kappa \sum_{F \in F^i} \langle \{\epsilon \nabla \eta^{j+1} \cdot n_F\}, [\xi^{j+1}] \rangle_F$$
$$+ \sum_{F \in F_{\mathrm{out}}^{\partial}} \langle \beta \xi^{j+1} \cdot n_F, \eta^{j+1} \rangle_F - (1 - \kappa) \sum_{F \in F^i} \langle \{\epsilon \nabla \eta^{j+1} \cdot n_F\}, [\eta^{j+1}] \rangle_F$$
$$+ \sum_{F \in F^i} |F|^{-1} \langle \sigma_F [\xi^{j+1}], [\eta^{j+1}] \rangle_F + e_c(u^{j+1}, \eta^{j+1}) + d(\xi^{j+1}, \eta^{j+1}) - d(\eta^{j+1}, \eta^{j+1}). \tag{4.14}$$

As the remainder of the proof is similar to the proof of Theorem 3.5, we only present the bounds for the first two terms in the right-hand side of (4.14). Using a Taylor expansion with integral remainder, we have

$$u^{*j} = u^{*j+1} - \Delta t \partial_t u^*(t^{j+1}) + \frac{1}{2} \int_{t^j}^{t^{j+1}} (s - t^j) \partial_{tt} u^*(s) ds.$$

This implies that

$$\|\partial_t u^*(t^{j+1}) - \frac{u^{*j+1}-u^{*j}}{\Delta t}\|_\Omega^2 \leq \frac{1}{2\Delta t^2}\int_{t^j}^{t^{j+1}}(s-t^j)^2 ds \int_{t^j}^{t^{j+1}} \|\partial_{tt}u^*\|_\Omega^2$$
$$\leq \frac{\Delta t}{6}\int_{t^j}^{t^{j+1}} \|\partial_{tt}u^*\|_\Omega^2. \tag{4.15}$$

Therefore, we have

$$(\partial_t u^*(t^{j+1}) - \frac{u^{*j+1}-u^{*j}}{\Delta t}, \eta^{j+1})_\Omega \leq \|\eta^{j+1}\|_\Omega^2 + C\Delta t^3 \int_{t^j}^{t^{j+1}} \|\partial_{tt}u^*\|_\Omega^2.$$

The second term in the right-hand side of (4.14) is bounded as

$$(\partial_t \xi(t^{j+1}), \eta^{j+1})_\Omega \leq \|\eta^{j+1}\|_\Omega^2 + C_a\, h^{2p}|\partial_t u^{j+1}|_{H^p(\Omega)}^2.$$

As in the derivation of the stability result, we need the time step to be small enough in order to conclude. A discrete Gronwall's lemma is used, and the rest of the proof is straightforward. ☐

REMARK 4.3. *If Condition II is not needed, then we can remove the constraint Δt small enough. However, we need that $\epsilon_* > 0$ and the constant C in the right-hand side of the resulting estimate will then additionally depend on ϵ^{-1}.*

4.2. Forward Euler time discretization. In this paper, we refer to the explicit DG solution as the solution defined by:

$$\forall v_h \in V_h, \quad (\frac{u_h^{j+1}-u_h^j}{\Delta t}, v_h) = L^j(v_h) - A(u_h^j, v_h), \tag{4.16}$$
$$\forall v_h \in V_h, \quad (u_h^0, v_h) = (u_0, v_h). \tag{4.17}$$

We first derive a stability bound.

THEOREM 4.4. *For $t > 0$, let $(u_h^j)_j$ be the discrete solution in V_h to (4.16)-(4.17) and assume that $a = a_1$ and for given $k = 1, 2, 3$, fix $d = d_k$. If $k = 3$ and $\tilde{\kappa} \in \{-1, 0\}$, assume that Condition I holds true. If $k = 1$, $\delta \neq 0$ and $\tilde{\kappa} \in \{-1, 0\}$, assume that Condition II holds true. Assume that Condition I holds true for $k = 2, \delta \neq 0$ and $\tilde{\kappa} \in \{-1, 0\}$. Then, $(u_h^j)_j$ satisfies the bound for all $n > 0$:*

$$\|u_h^n\|_\Omega^2 + C\Delta t \sum_{j=0}^{n-1} |||u_h^j|||_k^2 dt \leq \|u_0\|_\Omega^2 + C_{\tau,\epsilon^*}\Delta t \sum_{j=1}^{n}(\|f^j\|_\Omega^2 + \sum_{F\in F_{\text{in}}^\partial} \||\beta\cdot n_F|^{1/2} u_{\text{in}}^j\|_F^2) \tag{4.18}$$

where C_{τ,ϵ^*} is a constant independent of $h, \Delta t$ and ϵ_* but depending on C_τ and ϵ^*.

Proof. Choose $v_h = u_h^j$ in (4.16). We obtain a similar bound as in (3.13):

$$\frac{1}{2\Delta t}(\|u_h^{j+1}\|_\Omega^2 - \|u_h^j\|_\Omega^2) + \sum_{\Omega_e\in\mathcal{T}_h}\|\epsilon^{1/2}\nabla u_h^j\|_{\Omega_e}^2 + \frac{1}{2}\sum_{F\in F^i\cup F_{\rm HP}^i}\||\beta\cdot n_F|^{1/2}[u_h^j]\|_F^2$$
$$+\frac{1}{2}\sum_{F\in F_{\rm out}^\partial}\||\beta\cdot n_F|^{1/2}u_h^j\|_F^2 + \frac{1}{4}\sum_{F\in F_{\rm in}^\partial}\||\beta\cdot n_F|^{1/2}u_h^j\|_F^2$$
$$+\sum_{F\in F^i}|F|^{-1}\|\sigma_F^{1/2}[u_h^j]\|_F^2 + d(u_h^j,u_h^j) \le \sum_{F\in F_{\rm in}^\partial}\||\beta\cdot n_F|^{1/2}u_{\rm in}^j\|_F^2 + \frac{1}{4}\|f^j\|_\Omega^2$$
$$+\|u_h^j\|_\Omega^2 + |(1-\kappa)\sum_{F\in F_{\rm HP}^i}\langle\{\epsilon\nabla u_h^j\cdot n_F\},[u_h^j]\rangle_F|. \tag{4.19}$$

The remainder of the proof is similar to the Backward Euler case. □

To derive an error estimate for the forward Euler discretization, we will use the following lemma.

LEMMA 4.5. *There is a constant $C_b = C_{\epsilon^*,i,\beta,\tau}$ independent of h,δ and ϵ_* such that*

$$\forall v_h, w_h\in V_h,\quad A(v_h,w_h)\le C_b\,h^{-2}\|v_h\|_\Omega\|w_h\|_\Omega. \tag{4.20}$$

Proof. The proof is quite simple and mostly uses inverse inequality (3.8). □

THEOREM 4.6. *Let u be the solution of (2.1)-(2.4) and let $(u_h^j)_j\in V_h$ be the sequence of discrete solutions satisfying (4.16)-(4.17). Assume that $a=a_1$ and for given $k=1,2,3$, fix $d=d_k$. Assume that $u_0\in H^{p+1}(\Omega)$, $u\in L^\infty(0,T;H^{p+1}(\Omega))$ and $\partial_t u\in L^\infty(0,T;H^p(\Omega))$ and $\partial_{tt}u\in L^2((0,T)\times\Omega)$. If $\delta=1$, there is a constant C_0 independent of h and ϵ_* such that if $h^{-2}\Delta t\le C_0$, then there are constants $C, C_{b,a}$ independent of h,ϵ_* and δ such that*

$$\|u^n-u_h^n\|_\Omega^2 \le C\Delta t^2\int_0^T\|\partial_{tt}u\|_\Omega^2$$
$$+C_{b,a}h^{2p}\Big(|u_0|_{H^{p+1}(\Omega)}^2 + \Delta t\sum_{j=1}^{n-1}|u^j|_{H^{p+1}(\Omega)}^2 + \Delta t\sum_{j=0}^{n-1}|\partial_t u^j|_{H^p(\Omega)}^2\Big). \tag{4.21}$$

If $\delta\neq 1$, there is a constant C_0 independent of h, ϵ_* and δ such that if $h^{-2}\Delta t\le C_0$, then there are constants $C, C_{b,a}$ independent of h,ϵ_* and δ such that

$$\|u^n-u_h^n\|_\Omega^2 \le C\Delta t^2\int_0^T\|\partial_{tt}u\|_\Omega^2 + C_t(1-\delta)^2(\epsilon_H^\Delta h^{-1})^2\Delta t\sum_{j=0}^{n-1}\|u^j\|_{H^2(\Omega)}^2$$
$$+C_{b,a}h^{2p}\Big(|u_0|_{H^{p+1}(\Omega)}^2 + \Delta t\sum_{j=1}^{n-1}|u^j|_{H^{p+1}(\Omega)}^2 + \Delta t\sum_{j=0}^{n-1}|\partial_t u^j|_{H^p(\Omega)}^2\Big). \tag{4.22}$$

Proof. The error equation yields:

$$\frac{1}{2\Delta t}(\|\eta^{j+1}\|_\Omega^2 - \|\eta^j\|_\Omega^2) + A(\eta^j,\eta^{j+1}) = A(\xi^j,\eta^{j+1}) + e_c(u^j,\eta^{j+1})$$
$$+(\partial_t\xi(t^j),\eta^{j+1})_\Omega + (\partial_t u^*(t^j) - \frac{u^{*j+1}-u^{*j}}{\Delta t},\eta^{j+1}).$$

Using (4.20) and (3.9), we have

$$|A(\xi^j,\eta^{j+1})-A(\eta^j,\eta^{j+1})| \le C_b h^{-2}\|\eta^j\|_\Omega\|\eta^{j+1}\|_\Omega + C_{b,a}\, h^p|u^j|_{H^{p+1}(\Omega)}h^{-1}\|\eta^{j+1}\|_\Omega.$$

We also have, as in (4.15):

$$\|\partial_t u^*(t^j) - \frac{u^{*j+1}-u^{*j}}{\Delta t}\|_\Omega^2 \le C\Delta t\int_{t^j}^{t^{j+1}} \|\partial_{tt}u\|_\Omega^2.$$

Thus, we obtain for $\delta = 1$:

$$\frac{1}{2\Delta t}(\|\eta^{j+1}\|_\Omega^2 - \|\eta^j\|_\Omega^2) \le C_b\, h^{-2}\|\eta^j\|_\Omega^2 + C_b\,(h^{-2}+1)\|\eta^{j+1}\|_\Omega^2$$
$$+C_{b,a}\, h^{2p}(|u^j|^2_{H^{p+1}(\Omega)} + |\partial_t u^j|^2_{H^p(\Omega)}) + C\Delta t\int_{t^j}^{t^{j+1}} \|\partial_{tt}u\|_\Omega^2.$$

Multiply by $2\Delta t$ and sum from $j=0$ to $j=n-1$:

$$(1 - C_b\Delta t(h^{-2}+1))\|\eta^n\|_\Omega^2 - \|\eta^0\|_\Omega^2 \le C_b\Delta t(h^{-2}+1)\sum_{j=0}^{n-1}\|\eta^j\|_\Omega^2$$
$$+C_{b,a}\, h^{2p}\Delta t\sum_{j=0}^{n-1}(|u^j|^2_{H^{p+1}(\Omega)} + |\partial_t u^j|^2_{H^p(\Omega)}) + C\Delta t^2\int_0^T \|\partial_{tt}u\|_\Omega^2.$$

The final result is obtained using a discrete Gronwall's lemma. In the case where $\delta \neq 1$, the consistency error is bounded like (3.34)

$$e_c(u^j,\eta^{j+1}) \le \|\eta^{j+1}\|_\Omega^2 + C_t(1-\delta)^2(\epsilon_H^\Delta h^{-1})^2\|u^j\|^2_{H^2(\Omega)},$$

and the final estimate is

$$\|\eta^n\|_\Omega^2 \le \|\eta^0\|_\Omega^2 + C\Delta t^2\int_0^T \|\partial_{tt}u\|_\Omega^2$$
$$+C_{b,a}\, h^{2p}\Delta t\sum_{j=0}^{n-1}(|u^j|^2_{H^{p+1}(\Omega)} + |\partial_t u^j|^2_{H^p(\Omega)}) + C_t(1-\delta)^2(\epsilon_H^\Delta h^{-1})^2\Delta t\sum_{j=0}^{n-1}\|u^j\|^2_{H^2(\Omega)}.$$

□

5. Adaptive Fluxes. In this section, we propose a novel diffusive flux definition along the interface Γ_{HP} that is obtained as a weighted average of the standard NIPG/SIPG fluxes (d_3) and the upwind flux (d_2). We refer to this flux as an adaptive flux as its value may vary along the interface. Let the function θ be the ratio between ϵ_P and ϵ_H:

$$\forall x \in \Gamma_{\mathrm{HP}}, \quad \theta(x) = \frac{\epsilon_H(x)}{\epsilon_P(x)}.$$

The adaptive flux is defined as:

$$\forall u_h, v_h \in V_h, \quad \tilde{d}(u_h,v_h) = (1-\theta)d_2(u_h,v_h) + \theta d_3(u_h,u_h), \tag{5.1}$$

where for readibility, we recall the definition of d_2 and d_3:

$$d_2(u_h,v_h) = -\nu(u_h,v_h) + \tilde{\kappa}_2\nu(v_h,u_h) + j_{\tilde{\sigma}_2}(u_h,v_h),$$
$$d_3(u_h,v_h) = -\alpha(u_h,v_h) + \tilde{\kappa}_3\alpha(v_h,u_h) + j_{\tilde{\sigma}_3}(u_h,v_h).$$

The parameters in the definition of d_2 are chosen to be:

- either $\tilde{\kappa}_2 = 1$ and $\tilde{\sigma}_2 \in \{1, \epsilon_H\}$,
- or $\tilde{\kappa}_2 \in \{-1, 0\}$ and $\tilde{\sigma}_2 = \tilde{\sigma}_0$ with $\tilde{\sigma}_0$ large enough.

The parameters in the definition of d_3 are

- either $\tilde{\kappa}_3 = 1$ and $\tilde{\sigma}_3 \in \{1, \epsilon_H\}$,,
- or $\tilde{\kappa}_3 \in \{-1, 0\}$ and $\tilde{\sigma}_3 = \tilde{\sigma}_0$ with $\tilde{\sigma}_0$ large enough.

With these definitions, the scheme (2.8) is unconditionally stable.

THEOREM 5.1. *Assume that $a = a_1$ and $d = \tilde{d}$ defined above. The solution u_h in V_h of (2.8)-(2.9) satisfies the following estimate:*

$$\|u_h(T)\|_\Omega^2 + \int_0^T |||u_h|||^2 + \int_0^T \sum_{F \in F_{\rm HP}^i} |F|^{-1} \|(\theta\tilde{\sigma}_3 + (1-\theta)\tilde{\sigma}_2)^{1/2}[u_h]\|_F^2$$
$$\leq \|u_h(0)\|_\Omega^2 + C_{\tau,\epsilon^*} \int_0^T \left(\|f\|_\Omega^2 + \sum_{F \in F_{\rm in}^\partial} \||\beta \cdot n_F|^{1/2} u_{\rm in}\|_F^2 \right),$$

where C_{τ,ϵ^*} is a constant independent of h and ϵ_* but dependent on C_τ and ϵ^* whenever $(\tilde{\kappa}_3, \tilde{\kappa}_2) \neq (1,1)$.

Proof. We obtain as in Theorem 3.2, the inequality (3.13). We note that

$$d(u_h, u_h) = \theta((\tilde{\kappa}_3 - 1)\alpha(u_h, u_h) + j_{\tilde{\sigma}_3}(u_h, u_h)) + (1-\theta)((\tilde{\kappa}_2 - 1)\nu(u_h, u_h) + j_{\tilde{\sigma}_2}(u_h, u_h)).$$

If $\tilde{\kappa}_3 = \tilde{\kappa}_2 = 1$, then we obtain the bound:

$$\|u_h(T)\|_\Omega^2 + \int_0^T |||u_h|||^2 + \int_0^T \sum_{F \in F_{\rm HP}^i} |F|^{-1} \|(\theta\tilde{\sigma}_3 + (1-\theta)\tilde{\sigma}_2)^{1/2} u_h\|^2$$
$$\leq \|u_h(0)\|_\Omega^2 + C \left(\|f\|_\Omega^2 + \sum_{F \in F_{\rm in}^\partial} \||\beta \cdot n_F|^{1/2} u_{\rm in}\|_F^2 \right). \tag{5.2}$$

If $\tilde{\kappa}_3 = 1$ and $\tilde{\kappa}_2 \in \{-1, 0\}$, we have to bound

$$(1-\theta)(\tilde{\kappa}_2 - 1)\nu(u_h, u_h) \leq C_{\epsilon^*}(1-\theta) \sum_{F \in F_{\rm HP}^i} |F|^{-1/2} \|[u_h]\|_F |F|^{1/2} \|\epsilon_H^{1/2} \nabla u_h\|_F$$
$$\leq \frac{1}{16} \sum_{\Omega_e \subset \Delta_H} \|\epsilon_H^{1/2} \nabla u_h\|_{\Omega_e}^2 + C_{\tau,\epsilon^*}(1-\theta) \sum_{F \in F_{\rm HP}^i} |F|^{-1} \|[u_h]\|_F^2.$$

Assuming that $\tilde{\sigma}_2 \geq \tilde{\sigma}_0$ then the second term can be hidden in the right-hand side of (3.13) and we obtain the estimate (5.2). If $\tilde{\kappa}_3 \in \{-1, 0\}$ and $\tilde{\kappa}_2 = 1$, we use the bound (3.16) and we obtain (5.2) if $\tilde{\sigma}_3 \geq \tilde{\sigma}_0$. Finally, the case $\{\tilde{\kappa}_2, \tilde{\kappa}_3\} \in \{-1, 0\}$ is handled in a similar fashion; the bound (5.2) is derived assuming that $\tilde{\sigma}_2$ and $\tilde{\sigma}_3$ are both large enough constants. The final estimate is obtained then by integrating in time and using Gronwall's lemma. □

It is easy to see that the adaptive flux $\tilde{d}$ produces a consistent scheme. We next derive some semi-discrete a priori error estimates.

THEOREM 5.2. *Let u be the solution of (2.1)-(2.4) and for $t > 0$ let $u_h(t) \in V_h$ be the discrete solution of (2.8)-(2.9) with $a = a_1$ and $d = \tilde{d}$. Assume that $u_0 \in H^{p+1}(\Omega)$, $u \in L^2(0, T; H^{p+1}(\Omega))$ and $\partial_t u \in L^2(0, T; H^p(\Omega))$. There is a constant $C_{i,\tau,t,\beta,a,\sigma,\epsilon^*}$*

independent of h and ϵ such that

$$\|(u-u_h)(T)\|_\Omega^2 + \int_0^T |||u(t)-u_h(t)|||^2 dt + \int_0^T \sum_{F\in F^i_{\rm HP}} \|(\theta\tilde\sigma_3 + (1-\theta)\tilde\sigma_2)^{1/2}[u(t)-u_h(t)]\|_F^2 dt$$

$$\le C_{i,\tau,t,\beta,a,\sigma,\epsilon^*} h^{2p}\Big(|u_0|^2_{H^{p+1}(\Omega)} + \tilde C\int_0^t |u(t)|^2_{H^{p+1}(\Omega)}dt + \int_0^t |\partial_t u(t)|^2_{H^p(\Omega)}dt\Big), \quad (5.3)$$

where $\tilde C = 1 + \frac{\epsilon^*}{\min_{x\in\Delta_H}\epsilon(x)}$ for $\tilde\sigma_3 = \epsilon_H$ and $\tilde C = 1$ otherwise. The constant $C_{i,\tau,t,\beta,a,\sigma,\epsilon^*}$ also depends on $\tilde\sigma_0^{-1}$ if $\tilde\sigma_3 = \tilde\sigma_0$ or if $\tilde\sigma_2 = \tilde\sigma_0$.

Proof. Using the same notation and derivation as in the proof of Theorem 3.5, we obtain the following error (see (3.31)):

$$\frac{1}{2}\frac{d}{dt}\|\eta\|_\Omega^2 + \frac{3}{4}\sum_{\Omega_e\in\mathcal{T}_h}\|\epsilon^{1/2}\nabla\eta\|^2_{\Omega_e} + \frac{7}{8}\sum_{F\in F^i}|F|^{-1}\|\sigma_F^{1/2}[\eta]\|_F^2$$

$$+\frac{7}{16}\sum_{F\in F^i\cup F^i_{\rm HP}}\||\beta\cdot n_F|^{1/2}[\eta]\|_F^2 + \frac{1}{2}\sum_{F\in F^\partial_{\rm in}}\||\beta\cdot n_F|^{1/2}\eta\|_F^2 + \frac{7}{16}\sum_{F\in F^\partial_{\rm out}}\||\beta\cdot n_F|^{1/2}\eta\|_F^2$$

$$\le \|\eta\|_\Omega^2 + C_{i,\tau,t,\beta,a,\sigma,\epsilon^*}\,h^{2p}(|u|^2_{H^{p+1}(\Omega)} + |\partial_t u|^2_{H^p(\Omega)}) + \tilde d(\xi,\eta) - \tilde d(\eta,\eta). \quad (5.4)$$

The last two terms are reduced to

$$\tilde d(\xi,\eta) - \tilde d(\eta,\eta) = -\theta\alpha(\xi,\eta) - (1-\theta)\nu(\xi,\eta) + \theta(1-\tilde\kappa_3)\alpha(\eta,\eta)$$
$$+(1-\theta)(1-\tilde\kappa_2)\nu(\eta,\eta) - \sum_{F\in F^i_{\rm HP}}\langle(\theta\tilde\sigma_3 + (1-\theta)\tilde\sigma_2)[\eta],[\eta]\rangle_F.$$

The term $\theta\alpha(\xi,\eta)$ is bounded as in (3.42) if $\tilde\sigma_3\in\{1,\tilde\sigma_0\}$ and as in (3.43) if $\tilde\sigma_3 = \epsilon_H$. The term $(1-\theta)\nu(\xi,\eta)$ is bounded as:

$$(1-\theta)\nu(\xi,\eta) \le C_{t,a,\epsilon^*}h^{2p}|u|^2_{H^{p+1}(\Omega)} + \frac{1-\theta}{32}j_{\tilde\sigma_2}(\eta,\eta),$$

with the constant depending on $\tilde\sigma_0^{-1}$ if $\tilde\sigma_2 = \tilde\sigma_0$. Thus, if $\tilde\kappa_2 = \tilde\kappa_3 = 1$, we obtain (5.3) by integrating the resulting error inequality from 0 and T and by using Gronwall's lemma. If $\tilde\kappa_2\in\{-1,0\}$, the term $(1-\theta)(1-\tilde\kappa_2)\nu(\eta,\eta)$ is handled exactly as in (3.40). If $\tilde\kappa_3\in\{-1,0\}$, the term $\theta(1-\tilde\kappa_3)\alpha(\eta,\eta)$ is handled like (3.44). ∎

REMARK 5.3. *It is clear that we also obtain fully discrete estimates as in Section 4. If the time discretization is the backward Euler, then the stability bound (4.4) holds and the error estimate (4.8) is valid for $\tilde\sigma_3\neq\epsilon_H$ and (4.9) for the case $\tilde\sigma_3 = \epsilon_H$.*

6. Numerical Experiments.

6.1. Study of Fluxes. In this section, we investigate the numerical effect of the advective and diffusive fluxes listed in Section 2. We consider a simple test problem with large local Peclet number $Pe = \frac{\|\beta\|_{L^\infty}h}{2\epsilon}$ to highlight the difficulties associated with the calculation of the numerical approximation on regions from high to low diffusivity. Our domain is a two-dimensional rectangular domain $[0,2]\times[0,1]$ with a triangular mesh consisting of 200 elements displayed in Fig. 2.1. We impose noflow conditions on top and bottom boundaries, an inflow value of $u_{\rm in} = 1$ on the left boundary, and outflow on the right boundary. The initial solution consists of $u = 0$ everywhere in the domain. The velocity is $\beta = (1,0)$ and the source function f is zero.

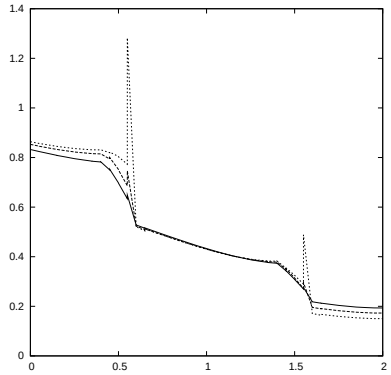

FIG. 6.1. *Explicit NIPG solution everywhere ($\kappa = 1$, $\sigma_F = 1$, $d = d_2$, $\tilde{\kappa} = 1$, $\tilde{\sigma}_F = 1$) for $Pe = 0.05$ (solid line), $Pe = 1$ (dashed line), and $Pe = 5$ (dotted line) in Ω_H at time $t_1 = 1.0$.*

Unless otherwise specified, the diffusion parameter is $\epsilon_P = 1$ on $\Omega_{\rm P}$ and $\epsilon_H = 10^{-3}$ on $\Omega_{\rm H}$ resulting in an abrubt jump from $\mathrm{Pe} = 0.05$ to $\mathrm{Pe} = 50$ at the interface $\Gamma_{\rm HP}$.

This particular test problem highlights the numerical difficulties encountered in modeling advection dominated regimes. The local Peclet number is sufficiently large to impose hyperbolic-type behavior in the solution, even in the non-degenerate diffusion case. It is well known that the presence of numerical oscillations in advection dominated regimes can be minimized by refining the mesh or equivalently, decreasing the local Peclet number. In our experiment, the spurious overshoot of the solution near the interface $\Gamma_{\rm HP}$ can be similarly diminished, as shown in Fig. 6.1 where, as a basis for comparison, we focus on the profile of the numerical solution along $\{(x, 0.5) : 0 \leq x \leq 2\}$. We implement the NIPG method everywhere ($\kappa = 1$, $\sigma_F = 1$, $d = d_2$, $\tilde{\kappa} = 1$, $\tilde{\sigma}_F = 1$) and employ a forward Euler scheme (4.16) - (4.17) with discontinuous piecewise linear basis functions. We vary the value of ϵ_H to demonstrate the corresponding numerical instability for increasing Peclet numbers at a fixed time $t_1 = 1.0$. Clearly Pe must be close to 1 or smaller to achieve minimal overshoot. However, such an equivalent refinement in the computational mesh for a fixed ϵ introduces a considerable computational cost that we aim to avoid while maintaining the integrity of the solution.

In an effort to minimize such instability, we explore various definitions of the flux at interface $\Gamma_{\rm HP}$. First, we consider several combinations of advective and diffusive fluxes consisting of upwind, average and downwind fluxes (Fig. 6.2, Fig. 6.3, Fig 6.4). With the exception of flux terms on the interface $\Gamma_{\rm HP}$, the underlying method is NIPG ($\kappa = 1, \sigma_F = 1$). On each figure, the profiles are shown at different times $t_0 = 0.4$ (solid line), $t_1 = 1.0$ (dashed line) and $t_2 = 2.0$ (dotted line). For Fig. 6.2, the advective flux is upwinded ($a = a_1$) and the diffusive flux takes several values: $d = -\nu$ (left figure), $d = -\alpha$ (center figure) and $d = d_4$ (right figure). The same choices of the diffusive flux are used in Fig. 6.3 ($a = a_2$) and Fig. 6.4 ($a = a_3$). These numerical studies show that, as expected, the best choice for the advective flux is upwinding. The average advective flux produces significant overshoot whereas the downwind advective flux yields unstable solutions. Consequently, throughout the rest of this paper, we fix the advective flux to be the upwind one.

From the analysis in Section 3, the case of upwind diffusive fluxes $d = -\nu$ produce stable solutions and optimal error estimates if Condition II holds true. However, this

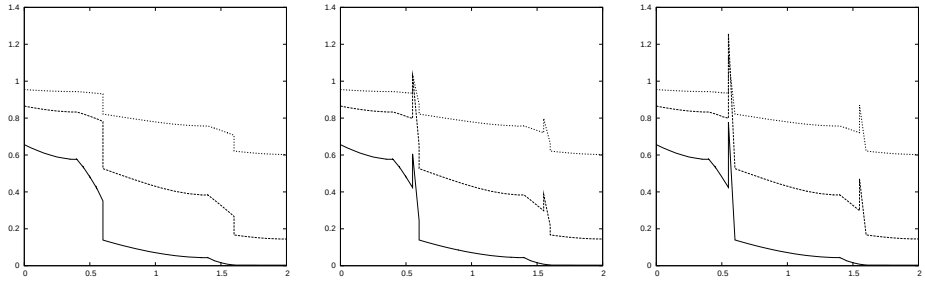

FIG. 6.2. *Explicit NIPG solution ($\kappa = 1, \sigma_F = 1$) for case $a = a_1$: upwind $d = -\nu$ (left), average $d = -\alpha$ (middle), downwind $d = d_4$ (right), at times t_0 (solid line), t_1 (dashed line) and t_2 (dotted line).*

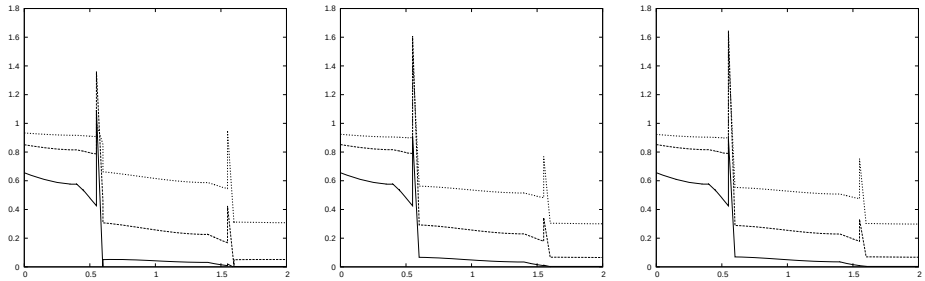

FIG. 6.3. *Explicit NIPG solution ($\kappa = 1, \sigma_F = 1$) for case $a = a_2$: upwind $d = -\nu$ (left), average $d = -\alpha$ (middle), downwind $d = d_4$ (right), at times t_0 (solid line), t_1 (dashed line) and t_2 (dotted line).*

means that this method does not converge as the mesh size tends to zero, even though Fig. 6.2 (left) looks satisfactory. Thus we investigate numerical diffusive flux definitions that produce a convergent solution as the mesh is uniformly refined. In Fig. 6.5, we display results obtained by repeating the same experiment but now consider the diffusive flux $d = d_2$ with $\tilde{\kappa} = 1$ and $\tilde{\sigma} \in \{1, \epsilon_H\}$ on Γ_{HP}. The overshoots are minimal if the penalty coefficient is upwinded ($j_{\tilde{\sigma}} = j_{\epsilon_H}$).

The numerical solution of the diffusive flux $d = d_2$ with penalty $\tilde{\sigma} = 1$ and $\tilde{\sigma} = 10$ are displayed in Fig. 6.6. Figures 6.7 and 6.8 contain results with diffusive flux $d = -\nu(u_h, v_h) + j_{\tilde{\sigma}}(u_h, v_h)$ and $d = -\alpha(u_h, v_h) + j_{\tilde{\sigma}}(u_h, v_h)$ respectively.

We now consider results obtains with the adaptive diffusive flux method described in Section 5. Fig. 6.9 displays the numerical solution for $d = \tilde{d}$ with $\tilde{\kappa}_3 = \tilde{\sigma}_3 = 1$ and differing choices for $\tilde{\kappa}_2$ and $\tilde{\sigma}_2$. All three figures are similar, yielding minimal overshoot near the interface Γ_{HP}. Fig. 6.10 shows the profile for $\tilde{\kappa}_3 = -1, \tilde{\sigma}_3 = 1$ and $\tilde{\kappa}_2 = \tilde{\sigma}_2 = 1$.

Next, we employ the SIPG method by selecting $\kappa = -1$ in (2.6) and vary the diffusive flux definition on Γ_{HP}. In this case, there is a constraint on the size of the penalty parameter σ_F. We repeat the experiment with zero diffusive flux ($d = 0$) on Γ_{HP} and observe in Fig. 6.11 that the parameter σ_F has to be chosen quite large ($\sigma_F = 100$) to obtain a stable solution. However, if the standard SIPG diffusive flux ($d = d_2$ with $\tilde{\kappa} = -1$) is used with an explicit time discretization, the solutions we obtain blow up even in the case of large penalty parameters and very small time steps.

In the remainder of this section, we employ an implicit in time discretization (4.2),

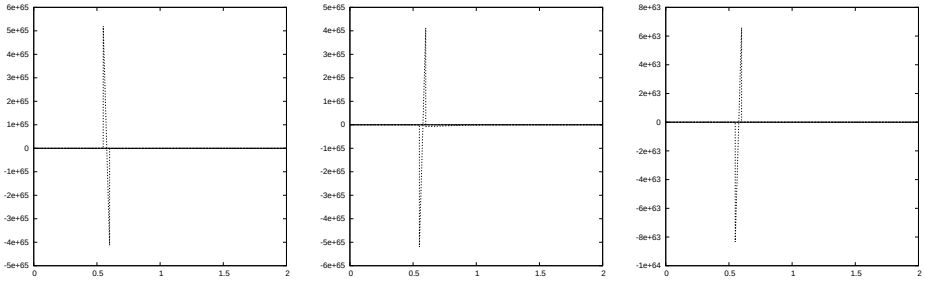

FIG. 6.4. *Explicit NIPG solution ($\kappa = 1, \sigma_F = 1$) for case $a = a_3$: upwind $d = -\nu$ (left), average $d = -\alpha$ (middle), downwind $d = d_4$(right), at times t_0 (solid line), t_1 (dashed line) and t_2 (dotted line).*

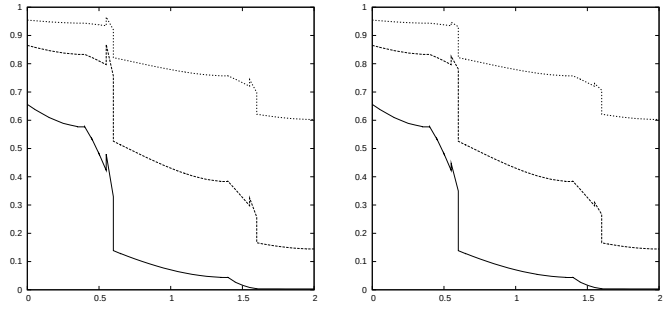

FIG. 6.5. *Explicit NIPG solution ($\kappa = 1, \sigma_F = 1$) for case $d = d_2$ with $\tilde{\kappa} = 1$: $\tilde{\sigma} = 1$ (left), $\tilde{\sigma} = \epsilon_H$ (right), at times t_0 (solid line), t_1 (dashed line) and t_2 (dotted line).*

(4.3) and vary the diffusive flux similarly as above. Additionally, we present solutions for both discontinuous piecewise linears and discontinuous piecewise quadratics basis functions. The time step is taken 20 times larger than for the forward Euler scheme. The NIPG method ($\kappa = 1, \sigma_F = 1$) is used in Fig. 6.12, Fig. 6.13 and Fig. 6.14 whereas the SIPG method ($\kappa = -1, \sigma_F = 10$) is shown in Fig. 6.15 and Fig. 6.16. It is not suprising to observe that whenever overshoot/oscillations occur, those phenomena are exacerbated when the polynomial degree is increased (Fig. 6.12, Fig. 6.15). However, in the case of no overshoot, increasing the degree does not affect the solution (Fig. 6.13, Fig. 6.14, Fig. 6.16). A comparison of the explicit and implicit solutions shows that in general, the backward Euler time discretization helps reduce the amount of overshoot/oscillations.

The conclusion of these numerical studies is that the best choices in the convergent methods described in Lemma 3.6 are

- $\kappa = \sigma_F = 1$ and $d(u_h, v_h) = -\nu(u_h, v_h) + \nu(v_h, u_h) + j_{\epsilon_H}(u_h, v_h)$
- $\kappa = \sigma_F = 1$ and $d(u_h, v_h) = \tilde{d}(u_h, v_h)$ with $\tilde{\kappa}_3 = \tilde{\sigma}_3 = 1$ and $\tilde{\kappa}_2 = 1, \tilde{\sigma}_2 = \epsilon_H$.

These methods produce very little overshoot and undershoot.

6.2. Convergence Rates. In this section, we present numerical rates of convergence for a variety of diffusive fluxes, that produce convergent methods according to the error estimates.

The domain Ω is the unit square with a coarse mesh of 25 square elements ($h = 0.2$), containing a subdomain $\Omega_H = [0.4, 0.6] \times [0, 1]$. The diffusion coefficients are constants $\epsilon_P = 1$ and ϵ_H takes the values 10^{-8} and 10^{-4}. We consider the following

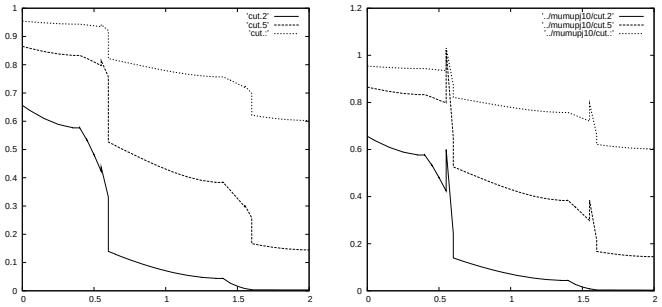

FIG. 6.6. *Explicit NIPG solution ($\kappa = 1, \sigma_F = 1$) with $d = d_2$: $\tilde{\kappa} = 1$ (left) and $\tilde{\kappa} = 10$ (right) at times t_0 (solid line), t_1 (dashed line) and t_2 (dotted line).*

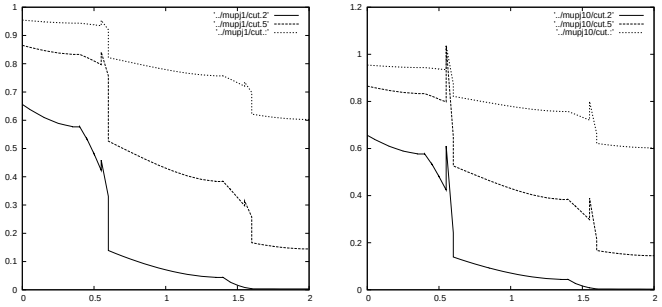

FIG. 6.7. *Explicit NIPG solution ($\kappa = 1, \sigma_F = 1$) with $d = -\nu(u_h, v_h) + j_{\tilde{\sigma}}(u_h, v_h)$: $\tilde{\kappa} = 1$ (left) and $\tilde{\kappa} = 10$ (right) at times t_0 (solid line), t_1 (dashed line) and t_2 (dotted line).*

smooth analytical solution:

$$\forall 0 \leq x \leq 0.4, \quad u(x) = \frac{\epsilon}{1.4 - 0.4\epsilon} x e^{x+t},$$

$$\forall 0.4 \leq x \leq 0.6, \quad u(x) = (x + 0.56\frac{\epsilon - 1}{1.4 - 0.4\epsilon})e^{x+t},$$

$$\forall 0.6 \leq x \leq 1.0, \quad u(x) = ((1.6\epsilon - 0.6 + \frac{0.56(\epsilon - 1)^2}{1.4 - 0.4\epsilon})x + 0.6 + (0.56\frac{\epsilon - 1}{1.4 - 0.4\epsilon}) - 0.6(1.6\epsilon - 0.6 + \frac{0.56(\epsilon - 1)^2}{1.4 - 0.4\epsilon}))e^{x+t}.$$

The coarse mesh is successively uniformly refined, each triangle being divided into four triangles at each refinement stage. The time step is chosen small enough so that the numerical error is of the order of the spatial approximation error. We present errors obtained with the backward Euler discretization. The convergence rate is obtained as $log(e_h/e_{h/2})/log(2)$ where e_h is the numerical error obtained on the mesh with size h. We compute both H_1^0 and L^2-type errors defined below:

$$E_1 = \frac{(\sum_{\Omega_e \in \mathcal{T}_h} \|\epsilon^{1/2} \nabla(u(T) - u_h(T))\|^2_{\Omega_e})^{1/2}}{(\sum_{\Omega_e \in \mathcal{T}_h} \|\epsilon^{1/2} \nabla u(T)\|^2_{\Omega_e})^{1/2}}$$

$$E_2 = \frac{(\sum_{\Omega_e \in \mathcal{T}_h} \|u(T) - u_h(T)\|^2_{\Omega_e})^{1/2}}{\sum_{\Omega_e \in \mathcal{T}_h} \|u(T)\|^2_{\Omega})^{1/2}}$$

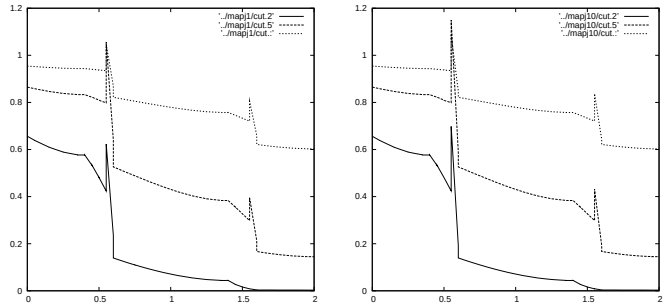

FIG. 6.8. *Explicit NIPG solution ($\kappa = 1, \sigma_F = 1$) with $d = -\alpha(u_h, v_h) + j_{\tilde{\sigma}}(u_h, v_h)$: $\tilde{\kappa} = 1$ (left) and $\tilde{\kappa} = 10$ (right) at times t_0 (solid line), t_1 (dashed line) and t_2 (dotted line).*

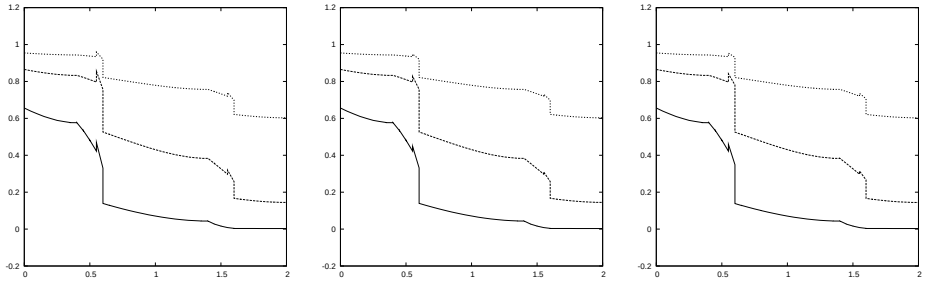

FIG. 6.9. *Explicit NIPG solution ($\kappa = 1, \sigma_F = 1$) for case $d = \tilde{d}$ with $\tilde{\kappa}_3 = \tilde{\sigma}_3 = 1$ and $\tilde{\kappa}_2 = 0$, $\tilde{\sigma}_2 = 1$ (left), or $\tilde{\kappa}_2 = -1, \tilde{\sigma}_2 = 1$ (middle), or $\tilde{\kappa}_2 = 1, \tilde{\sigma}_2 = \epsilon_H$ (right), at times t_0 (solid line), t_1 (dashed line) and t_2 (dotted line).*

Table 6.1 contains the numerical errors and the corresponding convergence rates for the case $\epsilon_H = 10^{-8}$ in the case of the NIPG method ($\kappa = \sigma_F = 1$) for several diffusive fluxes. The results for both discontinuous linear and quadratic approximations are presented. The convergence rates for the H_0^1 error ($\mathcal{O}(h^p)$) confirm the theoretical results. The rates for the L^2 error are optimal for piecewise linears and suboptimal for piecewise quadratics; this result is well-known for even polynomial degree for the NIPG method in general and remains an open question.

Table 6.2 presents the errors and convergence rates in the case of the SIPG method ($\kappa = -1, \sigma_F = 10$). In this case, the choice $\sigma_F = 1$ will not yield optimal rates. Using the jump parameter $\sigma_F = 10$, we obtain optimal rates for both polynomial degrees and both norms.

Finally, we repeat the same experiments for a larger $\epsilon_H = 10^{-4}$ in Table 6.3.

6.3. Randomized diffusion. In this test problem, the diffusion coefficient is randomly selected to be either $\epsilon = 1$ or $\epsilon = 10^{-3}$ on each individual element (see Fig. 6.17) using a random number generator. The velocity vector is $\beta = (1, 1)$, and consequently the inflow boundary consists of the left vertical boundary and bottom horizontal boundary. A forward Euler in time and piecewise linear discretization is used in this case. First, we compare the standard NIPG solution ($d = d_3$ and $\kappa = \sigma_F = \tilde{\sigma} = 1$) with the improved NIPG solution ($\kappa = 1, \sigma_F = 1$) obtained by employing a diffusion coefficient of upwinded type, $d(u_h, v_h) = -\nu(u_h, v_h) + \nu(v_h, u_h) + j_{\epsilon_H}(u_h, v_h)$. The profiles of the solution extracted along the line $\{(x, 0.45) : 0 \le x \le 2\}$ are shown in Fig.6.18. Clearly the NIPG method blows up after some finite time whereas the

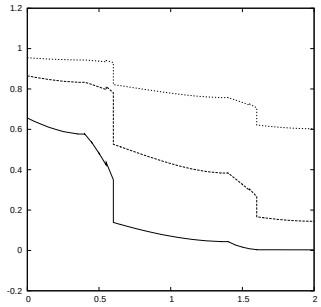

FIG. 6.10. *Explicit NIPG solution ($\kappa = 1, \sigma_F = 1$) for case $d = \tilde{d}$ with $\tilde{\kappa}_3 = -1$, $\tilde{\sigma}_3 = 1$ and $\tilde{\kappa}_2 = \tilde{\sigma}_2 = 1$, at times t_0 (solid line), t_1 (dashed line) and t_2 (dotted line).*

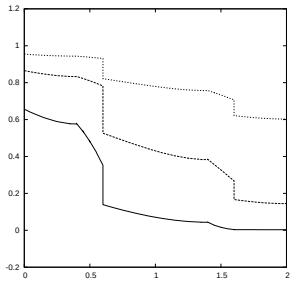

FIG. 6.11. *Explicit SIPG solution ($\kappa = -1, \sigma_F = 100$) with zero diffusive flux ($d = 0$) at times t_0 (solid line), t_1 (dashed line) and t_2 (dotted line).*

improved NIPG is stable. In order to better see the improved NIPG profiles, we show them again in Fig. 6.19, with the profiles obtained with the adaptive NIPG method ($d = \tilde{d}$ with $\tilde{\kappa}_2 = \tilde{\kappa}_3 = \tilde{\sigma}_3 = 1, \tilde{\sigma}_2 = \epsilon_H$). Two dimensional contours of the solution for all three methods (standard, improved and adaptive NIPG) are shown in Fig. 6.20, 6.21 and Fig. 6.22 respectively.

7. Conclusions. In this paper we analyze and develop discontinuous Galerkin methods for an advection-diffusion equation with spatially varying diffusion coefficient. Without resorting to slope limiting techniques nor mesh refinement, we demonstrate successful choices of numerical fluxes that appropriately capture solution behavior by eliminating the overshoot phenomena occuring naturally with the standard DG methods. We derived stability and a prior error estimates, obtaining optimality for both the continuous and discrete time discretizations. Numerical tests indicate the robustness of our convergence estimates. Moreover, our numerical results indicate a substantial improvement in the solution for our adaptive flux technique over standard DG flux definitions. Extensions of this work to nonlinear transport problems are currently under investigation.

REFERENCES

[1] V. Aizinger, C.N. Dawson, B. Cockburn, and P. Castillo. The local discontinuous Galerkin method for contaminant transport. *Advances in Water Resources*, 24:73–87, 2000.

[2] D.N. Arnold. An interior penalty finite element method with discontinuous elements. *SIAM J. Numer. Anal.*, 19:742–760, 1982.

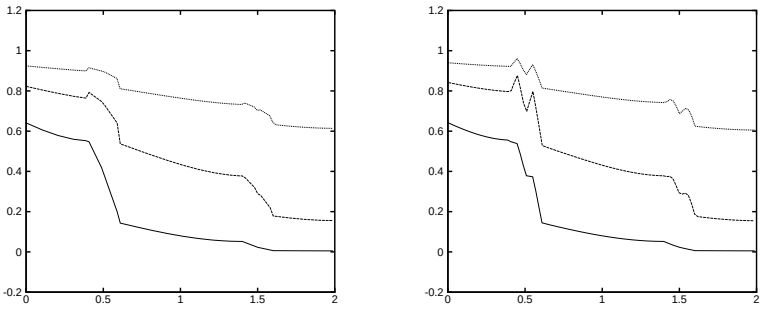

FIG. 6.12. *Implicit NIPG solution* ($\kappa = 1, \sigma_F = 1$) *:* $p = 1$ *(left) and* $p = 2$ *(right), at times* t_0 *(solid line),* t_1 *(dashed line) and* t_2 *(dotted line).*

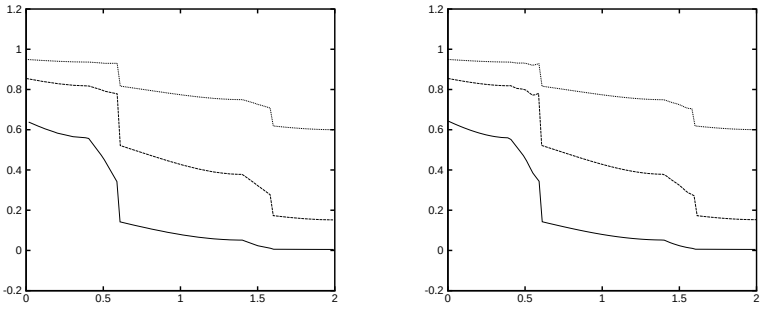

FIG. 6.13. *Implicit NIPG solution* ($\kappa = 1, \sigma_F = 1$) *with* $d = d_2$ *and* $\tilde{\sigma} = \epsilon_H$*:* $p = 1$ *(left) and* $p = 2$ *(right), at times* t_0 *(solid line),* t_1 *(dashed line) and* t_2 *(dotted line).*

[3] C.E. Baumann and J.T. Oden. A discontinuous hp finite element method for convection-diffusion problems. *Computer Methods Appl. Mech. Engrg.*, 175 (3-4):311–341, 1999.

[4] J. Bea and Y. Bachmat. *Introduction to Modeling of Transport Phenomena in Porous Media*. Kluwer Academic Publishers, London, 1991.

[5] S.C. Brenner and L.R. Scott. *The Mathematical Theory of Finite Element Methods*, volume Texts in Applied Mathematics Vol. 15. Springer-Verlag, 1984.

[6] P. Castillo, B. Cockburn, D. Schötzau, and C. Schwab. An optimal a priori error estimate for the hp-version of the local discontinuous Galerkin method for convection-diffusion problems. *Mathematics of Computation*, 71(238):455–478, 2002.

[7] G. Chavent and J. Jaffré. *Mathematical Models and Finite Elements for Reservoir Simulation*. North-Holland, Amsterdam, 1986.

[8] B. Cockburn and C.N. Dawson. Some extensions of the local discontinuous Galerkin method for convection-diffusion equations in multidimensions. In J. Whiteman, editor, *Mathematics of Finite Elements and Applications: MAFELAP X*, pages 264–285. Elsevier, 2000.

[9] B. Cockburn and C.-W. Shu. The local discontinuous Galerkin method for time-dependent convection-diffusion systems. *SIAM J. Numer. Anal.*, 35:2440–2463, 1998.

[10] J.-P. Croisille, A. Ern, T. Lelièvre, and J. Proft. Analysis and simulation of a coupled hyperbolic/parabolic model problem. *Journal of Numerical Mathematics*, 13(2):81–103, 2005.

[11] C. Dawson and J. Proft. A priori error estimates for interior penalty versions of local discontinuous Galerkin methods applied to transport equations. *Numer. Methods in Partial Differential Equations*, 17(6):545–564, 2001.

[12] C. Dawson, S. Sun, and M.F. Wheeler. Compatible algorithms for coupled flow and transport. *Comput. Meth. Appl. Mech. Eng.*, 193:2565–2580, 2004.

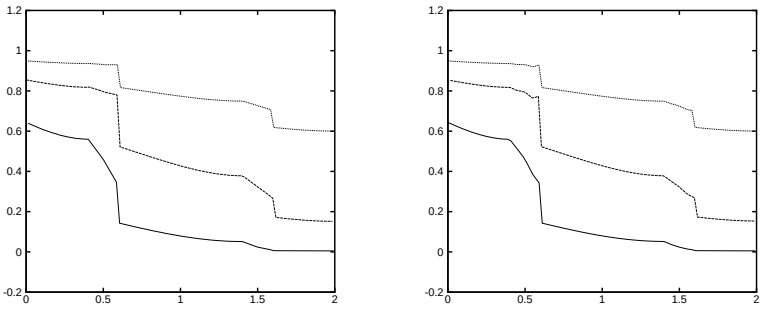

FIG. 6.14. *Implicit NIPG solution ($\kappa = 1, \sigma_F = 1$) with adaptive flux $d = \tilde{d}$ ($\tilde{\kappa}_2 = 1, \tilde{\sigma}_2 = \epsilon_H, \tilde{\kappa}_3 = \tilde{\sigma}_3 = 1$): $p = 1$ (left) and $p = 2$ (right), at times t_0 (solid line), t_1 (dashed line) and t_2 (dotted line).*

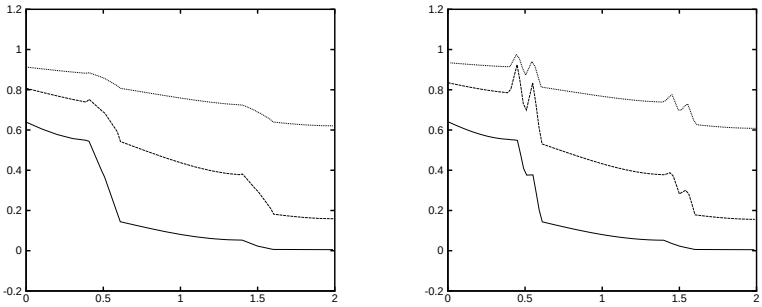

FIG. 6.15. *Implicit SIPG solution ($\kappa = -1, \sigma_F = 10$): $p = 1$ (left) and $p = 2$ (right), at times t_0 (solid line), t_1 (dashed line) and t_2 (dotted line).*

[13] A. Ern and J.-L. Guermond. *Theory and Practice of Finite Elements*, chapter Applied Mathematical Series Vol. 159. Springer-Verlag, 2004.

[14] A. Ern and J. Proft. Multi-algorithmic methods for coupled hyperbolic-parabolic problems. *International Journal of Numerical Analysis and Modeling*, 3(1):94–114, 2004.

[15] Y. Esphteyn and B. Rivière. Estimation of penalty parameters for symmetric interior penalty galerkin methods. submitted, also University of Pittsburgh technical report TR-MATH 06-05, 2006.

[16] R.E. Ewing. *The mathematics of Reservoir Simulation*, volume 1. Frontiers in Applied Mathematics, 1983.

[17] A. Frati, F. Pasquarelli, and A. Quarteroni. Spectral approximation to advection-diffusion problems by the fictitious interface method. *J. comput. Phys.*, 107:201–212, 1993.

[18] F. Gastaldi and A. Quarteroni. On the coupling of hyperbolic and parabolic systems: Analytical and numerical approach. *Appl. Numer. Math.*, 6:3–31, 1989.

[19] P. Houston, C. Schwab, and E. Süli. Discontinuous hp-finite element methods for advection-diffusion problems. *SIAM J. Numer. Anal.*, 39(6):2133–2163, 2002.

[20] P. Houston, C. Schwab, and E. Suli. Stabilized hp-finite element methods for first-order hyperbolic problems. *SIAM J. Numer. Anal.*, 37:1618–1643, 2000.

[21] J. Douglas Jr. and T.F. Russell. Numerical methods for convection-diffusion problems based on combining the method of characteristics with finite element or finite difference procedures. *SIAM J. Numer. Anal.*, 19:871–885, 1982.

[22] B. Rivière and M.F. Wheeler. Discontinuous Galerkin methods for flow and transport problems in porous media. *Communications in Numerical Methods in Engineering*, 18:63–68, 2002.

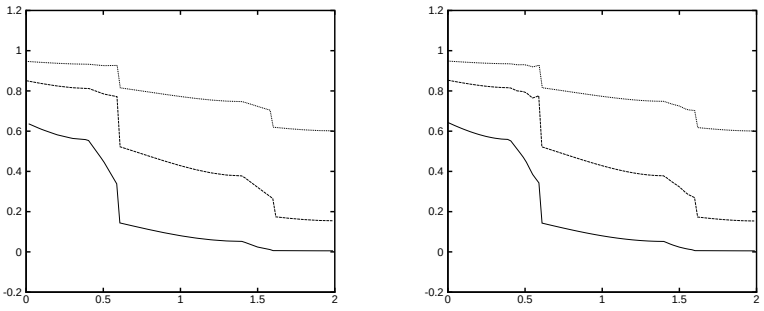

FIG. 6.16. *Implicit SIPG solution with* ($\kappa = -1, \sigma_F = 10$) *and adaptive flux* $d = \tilde{d}$ ($\tilde{\kappa}_2 = 1, \tilde{\sigma}_2 = \epsilon_H, \tilde{\kappa}_3 = \tilde{\sigma}_3 = 1$)*:* $p = 1$ *(left) and* $p = 2$ *(right), at times* t_0 *(solid line),* t_1 *(dashed line) and* t_2 *(dotted line).*

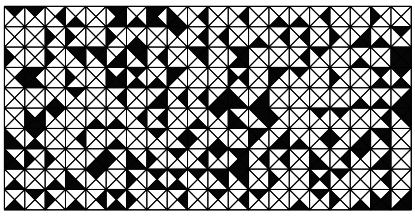

FIG. 6.17. *Mesh and diffusion coefficient randomly generated* ($\epsilon_P = 1$ *white,* $\epsilon_H = 10^{-3}$ *gray).*

[23] B. Rivière and M.F. Wheeler. Nonconforming methods for transport with nonlinear reaction. *Contemporary Mathematics*, 295:421–432, 2002.

[24] B. Rivière, M.F. Wheeler, and V. Girault. Improved energy estimates for interior penalty, constrained and discontinuous Galerkin methods for elliptic problems, part I. *Computational Geosciences*, 3:337–360, 1999.

[25] B. Rivière, M.F. Wheeler, and V. Girault. A priori error estimates for finite element methods based on discontinuous approximation spaces for elliptic problems. *SIAM J. Numer. Anal.*, 39(3):901–931, 2001.

[26] P. Siegel, R. Mosé, P. Ackerer, and J. Jaffre. Solution of the advection-diffusion equation using a combination of discontinuous and mixed finite elements. *Intl. J. Numer. Meth. Flu.*, 24:595–613, 1997.

[27] S. Sun, B. Rivière, and M.F. Wheeler. A combined mixed finite element and discontinuous Galerkin method for miscible displacement problems porous media. *Proceedings of International Symposium on Computational and Applied PDEs*, pages 321–348, 2002.

[28] S. Sun and M.F. Wheeler. Discontinuous Galerkin methods for coupled flow and reactive transport problems. *Applied Numerical Mathematics*, 52(2-3):273–298, 2005.

[29] S. Sun and M.F. Wheeler. Symmetric and nonsymmetric discontinuous Galerkin methods for reactive transport in porous media. *SIAM J. Numerical Analysis*, 43(1):195–219, 2005.

[30] R.L. Trotta. Multidomain finite elements for advection-diffusion equations. *Appl. Numer. Math.*, 21:91–118, 1996.

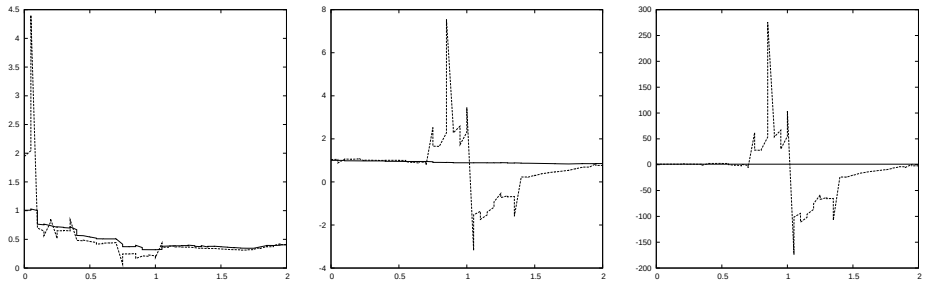

FIG. 6.18. *Comparison between standard NIPG (dashed line, $\kappa = \sigma_F = \tilde{\kappa} = \tilde{\sigma} = 1$) and improved NIPG (solid line, $d = d_2$ with $\kappa = \sigma_F = \tilde{\kappa} = 1, \tilde{\sigma} = \epsilon_H$) at times t_0 (left), t_1 (middle) and t_2 (right).*

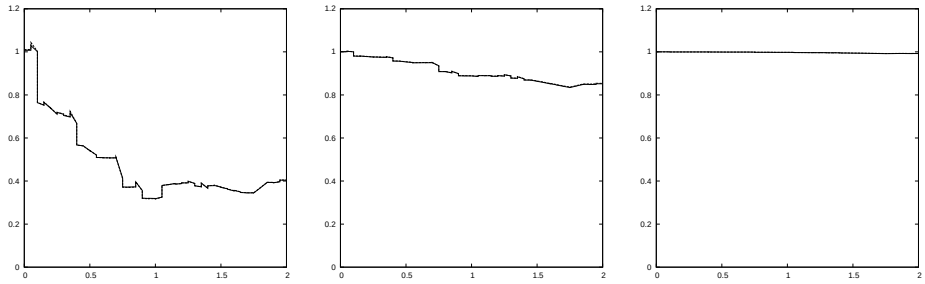

FIG. 6.19. *Comparison between upwinded flux (dashed line, $d = d_2$ with $\tilde{\kappa} = 1, \tilde{\sigma} = \epsilon_H$) and adaptive flux (solid line, $d = \tilde{d}$ with $\tilde{\kappa}_2 = \tilde{\kappa}_3 = \tilde{\sigma}_e = 1$, $\tilde{\sigma}_2 = \epsilon_H$) solutions at at times t_0 (left), t_1 (middle) and t_2 (right).*

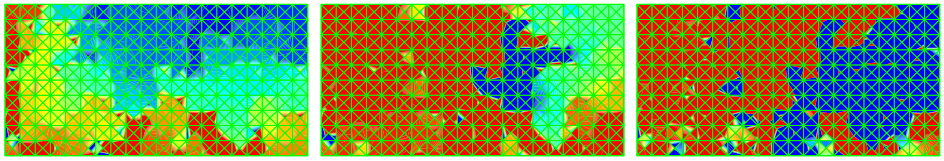

FIG. 6.20. *Two-dimensional contours with standard NIPG only ($\kappa = 1, \sigma_F = 1, \tilde{\kappa} = 1, \tilde{\sigma} = 1$), at times t_0 (left), t_1 (middle) and t_2 (right).*

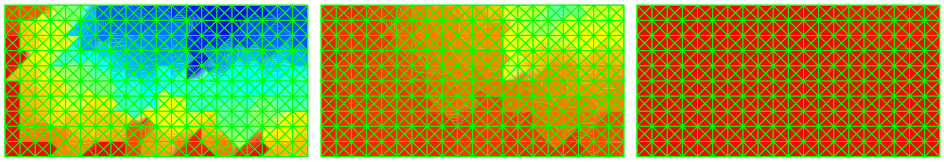

FIG. 6.21. *Two-dimensional contours with improved NIPG ($\kappa = 1, \sigma_F = 1, \tilde{\kappa} = 1, \tilde{\sigma} = \epsilon_H$, at times t_0 (left), t_1 (middle) and t_2 (right).*

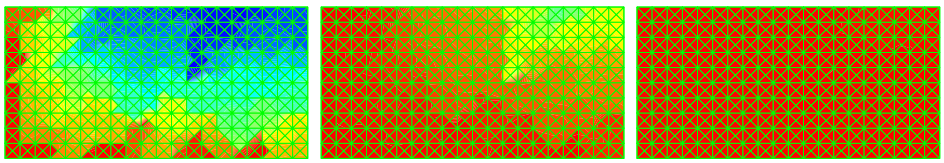

FIG. 6.22. *Two-dimensional contours with adaptive diffusive flux ($\kappa = 1, \sigma_F = 1, \tilde{\kappa}_2 = 1, \tilde{\sigma}_2 = \epsilon_H, \tilde{\kappa}_3 = 1, \tilde{\sigma}_3 = 1$, at times t_0 (left), t_1 (middle) and t_2 (right).*

Degree	h	E_1 error	E_1 rate	E_2 error	E_2 rate
		$d(u_h, v_h) = -\nu(u_h, v_h) + \nu(v_h, u_h) + j_1(u_h, v_h)$			
1	0.0125	1.7545447×10^{-2}	1.0015	4.2073064×10^{-5}	2.0739
2	0.025	2.7647501×10^{-4}	2.0011	1.5691227×10^{-6}	2.3730
		$d(u_h, v_h) = -\nu(u_h, v_h) + \nu(v_h, u_h) + j_{\epsilon_H}(u_h, v_h)$			
1	0.0125	1.7545095×10^{-2}	1.0006	3.9952727×10^{-5}	2.0274
2	0.025	2.7595571×10^{-4}	1.9945	1.5473538×10^{-6}	2.3567
		$d(u_h, v_h) = \tilde{d}(u_h, v_h)$ with $\tilde{\sigma}_2 = \epsilon_H$			
1	0.0125	1.7545095×10^{-2}	1.0006	3.9952728×10^{-5}	2.0274
2	0.025	2.7595571×10^{-4}	1.9945	1.5473538×10^{-6}	2.3567
		$d(u_h, v_h) = -\nu(u_h, v_h) + j_1(u_h, v_h)$			
1	0.0125	1.7545447×10^{-2}	1.0015	4.2073064×10^{-5}	2.0739
2	0.025	2.7647501×10^{-4}	2.0011	1.5691227×10^{-6}	2.3730
		$d(u_h, v_h) = -\nu(u_h, v_h) - \nu(v_h, u_h) + j_1(u_h, v_h)$			
1	0.0125	1.7545447×10^{-2}	1.0015	4.2073064×10^{-5}	2.0739
2	0.025	2.7647501×10^{-4}	2.0011	1.5691227×10^{-6}	2.3730
		$d(u_h, v_h) = -\alpha(u_h, v_h) + \alpha(v_h, u_h) + j_1(u_h, v_h)$			
1	0.0125	1.7555680×10^{-2}	1.0026	4.1100064×10^{-5}	2.0600
2	0.025	2.7642468×10^{-4}	2.0004	1.6135493×10^{-6}	2.4234
		$d(u_h, v_h) = -\alpha(u_h, v_h) - \alpha(v_h, u_h) + j_1(u_h, v_h)$			
1	0.0125	1.7569438×10^{-2}	1.0019	4.1109901×10^{-5}	2.0600
2	0.025	5.9608951×10^{-4}	1.5751	1.9646799×10^{-6}	2.4105
		$d(u_h, v_h) = -\alpha(u_h, v_h) + j_1(u_h, v_h)$			
1	0.0125	1.7569438×10^{-2}	1.0011	4.1109901×10^{-5}	2.0598
2	0.025	2.7670699×10^{-4}	2.0068	1.6059571×10^{-6}	2.4446

TABLE 6.1

Case $\epsilon_H = 10^{-8}$: NIPG everywhere ($\kappa = 1, \sigma_F = 1$) except on interface Γ_{HP}.

Degree	h	E_1 error	E_1 rate	E_2 error	E_2 rate
		$d(u_h, v_h) = -\nu(u_h, v_h) + \nu(v_h, u_h) + j_1(u_h, v_h)$			
1	0.0125	1.7545660×10^{-2}	1.0016	4.2126190×10^{-5}	2.0767
2	0.025	2.1164124×10^{-4}	2.0084	9.1280669×10^{-7}	2.9124
		$d(u_h, v_h) = -\nu(u_h, v_h) + \nu(v_h, u_h) + j_{\epsilon_H}(u_h, v_h)$			
1	0.0125	1.7545144×10^{-2}	1.0006	3.9950091×10^{-5}	2.0291
2	0.025	2.1150384×10^{-4}	2.0035	$8.8318117 \times 10^{-07}$	2.8742
		$d(u_h, v_h) = \tilde{d}(u_h, v_h)$ with $\tilde{\sigma}_2 = \epsilon_H$			
1	0.0125	1.7544665×10^{-2}	1.0000	4.8042199×10^{-5}	1.8989
2	0.025	2.1150384×10^{-4}	2.0035	8.8318117×10^{-7}	2.8742
		$d(u_h, v_h) = -\nu(u_h, v_h) + j_{10}(u_h, v_h)$			
1	0.0125	1.7545614×10^{-2}	1.0014	4.2126267×10^{-5}	2.0837
2	0.025	2.1163346×10^{-4}	2.0081	9.1349854×10^{-7}	2.9195
		$d(u_h, v_h) = -\nu(u_h, v_h) - \nu(v_h, u_h) + j_{10}(u_h, v_h)$			
1	0.0125	1.7545614×10^{-2}	1.0014	4.2126267×10^{-5}	2.0837
2	0.025	2.1163346×10^{-4}	2.0081	9.1349854×10^{-7}	2.9195
		$d(u_h, v_h) = -\alpha(u_h, v_h) + \alpha(v_h, u_h) + j_1(u_h, v_h)$			
1	0.0125	1.7560381×10^{-2}	1.0010	4.7968282×10^{-5}	1.9017
2	0.025	2.1297624×10^{-4}	2.0209	9.3458123×10^{-7}	2.9505
		$d(u_h, v_h) = -\alpha(u_h, v_h) - \alpha(v_h, u_h) + j_{10}(u_h, v_h)$			
1	0.0125	1.7545866×10^{-2}	1.0012	4.2060722×10^{-5}	2.0823
2	0.025	2.1157153×10^{-4}	2.0075	9.1485182×10^{-7}	2.9218
		$d(u_h, v_h) = -\alpha(u_h, v_h) + j_{10}(u_h, v_h)$			
1	0.0125	1.7545582×10^{-2}	1.0013	4.2014424×10^{-5}	2.0817
2	0.025	2.1164124×10^{-4}	2.0084	9.1607522×10^{-7}	2.9235

TABLE 6.2

Case $\epsilon_H = 10^{-8}$: SIPG everywhere ($\kappa = -1, \sigma_F = 10$) except on interface Γ_{HP}.

Degree	h	E_1 error	E_1 rate	E_2 error	E_2 rate
		$d(u_h, v_h) = -\nu(u_h, v_h) + \nu(v_h, u_h) + j_1(u_h, v_h)$			
1	0.0125	1.7479107×10^{-2}	1.0015	4.2054623×10^{-5}	2.0739
2	0.025	2.7532551×10^{-4}	2.0010	1.5675376×10^{-6}	2.3734
		$d(u_h, v_h) = -\nu(u_h, v_h) + \nu(v_h, u_h) + j_{\epsilon_H}(u_h, v_h)$			
1	0.0125	1.7478505×10^{-2}	1.0006	$3.9930289\,10^{-5}$	2.0277
2	0.025	2.7479793×10^{-4}	1.9945	$1.5462065\,10^{-6}$	2.3568
		$d(u_h, v_h) = \tilde{d}(u_h, v_h)$ with $\tilde{\sigma}_2 = \epsilon_H$			
1	0.0125	1.7478508×10^{-2}	1.0006	3.9931765×10^{-5}	2.0276
2	0.025	2.7479957×10^{-4}	1.9945	1.5461667×10^{-6}	2.3568
		$d(u_h, v_h) = -\nu(u_h, v_h) + j_1(u_h, v_h)$			
1	0.0125	1.7479107×10^{-2}	1.0015	4.2054591×10^{-5}	2.0739
2	0.025	2.7532574×10^{-4}	2.0010	1.5675166×10^{-6}	2.3734
		$d(u_h, v_h) = -\nu(u_h, v_h) - \nu(v_h, u_h) + j_1(u_h, v_h)$			
1	0.0125	1.7479107×10^{-2}	1.0015	4.2054559×10^{-5}	2.0739
2	0.025	2.7532598×10^{-4}	2.0010	1.5674956×10^{-6}	2.3733
		$d(u_h, v_h) = -\alpha(u_h, v_h) + \alpha(v_h, u_h) + j_1(u_h, v_h)$			
1	0.0125	1.7489212×10^{-2}	1.0027	4.1085319×10^{-5}	2.0600
2	0.025	2.7528374×10^{-4}	2.0004	1.6117432×10^{-6}	2.4239
		$d(u_h, v_h) = -\alpha(u_h, v_h) - \alpha(v_h, u_h) + j_1(u_h, v_h)$			
1	0.0125	1.7502868×10^{-2}	1.0019	4.1094792×10^{-5}	2.0600
2	0.025	5.9351950×10^{-4}	1.5745	1.9628641×10^{-6}	2.4104
		$d(u_h, v_h) = -\alpha(u_h, v_h) + j_1(u_h, v_h)$			
1	0.0125	1.7478734×10^{-2}	1.0011	4.1081056×10^{-5}	2.0598
2	0.025	2.7556932×10^{-4}	2.0067	1.6041858×10^{-6}	2.4451

TABLE 6.3

Case $\epsilon_H = 10^{-4}$: NIPG everywhere ($\kappa = 1, \sigma_F = 1$) except on interface Γ_{HP}.